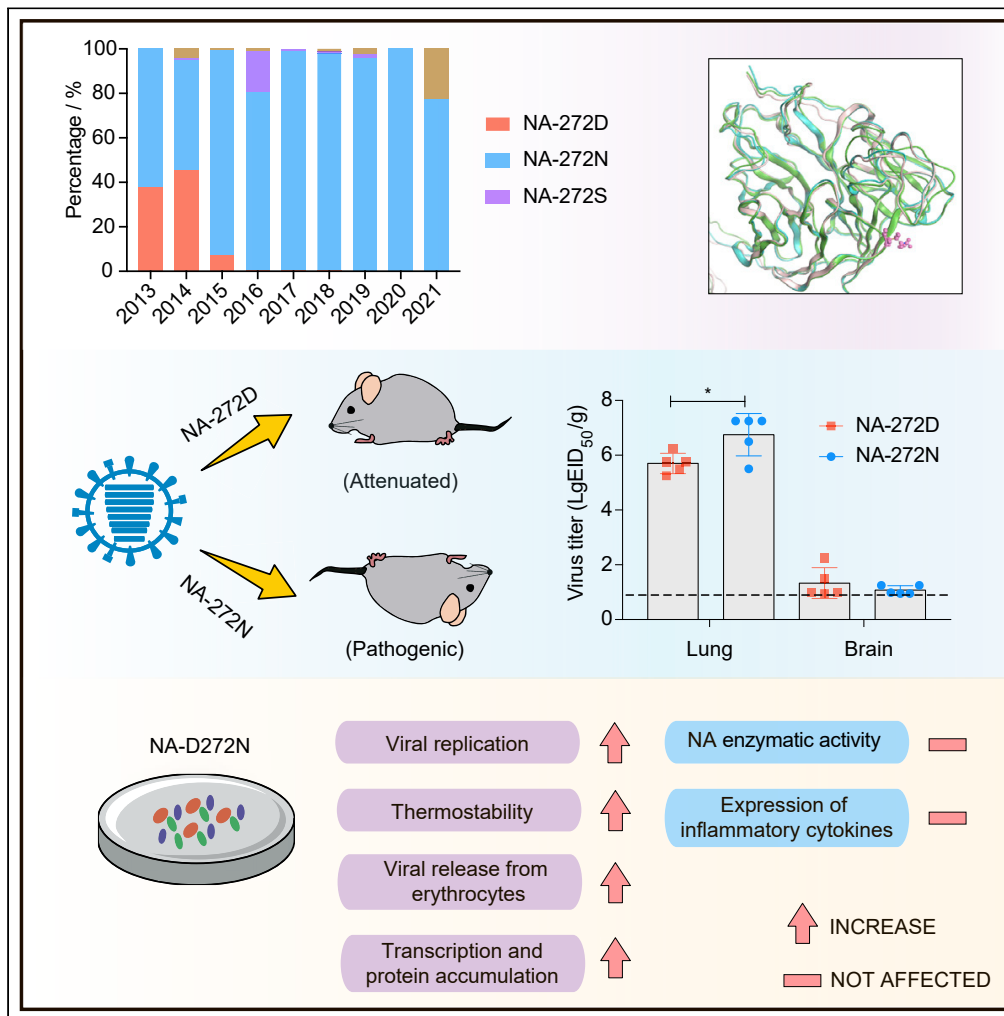


Article

Key amino acid position 272 in neuraminidase determines the replication and virulence of H5N6 avian influenza virus in mammals



Jiahao Zhang,
Xiaomin Wang,
Shiping Ding, ...,
Huanan Li, Ming
Liao, Wenbao Qi

mliao@scau.edu.cn (M.L.)
qiwenbao@scau.edu.cn (W.Q.)

Highlights

NA-D272N mutation of H5N6 became predominant in birds and humans since 2015

NA-D272N mutation significantly increased replication and virulence in mice

NA-D272N mutation increased viral release from erythrocytes and thermostability

NA-N272S mutation induced higher levels of inflammatory cytokines in human cells



Article

Key amino acid position 272 in neuraminidase determines the replication and virulence of H5N6 avian influenza virus in mammals

Jiahao Zhang,^{1,2,4,6} Xiaomin Wang,^{1,2,4,6} Shiping Ding,^{1,2,4} Kaixiong Ma,^{2,4} Yuting Jiang,^{1,2,4} Yang Guo,^{1,2,4} Tao Zhang,^{1,2,4} Yi Liu,^{1,2,4} Huanan Li,^{1,2,4} Ming Liao,^{2,3,4,5,*} and Wenbao Qi^{1,2,3,4,5,7,*}

SUMMARY

Avian influenza H5N6 virus not only wreaks economic havoc in the poultry industry but also threatens human health. Strikingly, as of August 2022, 78 human beings were infected with H5N6, and the spike in the number of human infections with H5N6 occurred during 2021. In the life cycle of influenza virus, neuraminidase (NA) has numerous functions, especially viral budding and replication. Here, we found that NA-D272N mutation became predominant in H5N6 viruses since 2015 and significantly increased the viral replication and virulence in mice. D272N mutation in NA protein increased viral release from erythrocytes, thermostability, early transcription, and accumulation of NA protein. Particularly, the dominant 272 residue switch from N to S has occurred in wild bird-origin H5N6 viruses since late 2016 and N272S mutation induced significantly higher levels of inflammatory cytokines in infected human cells. Therefore, comprehensive surveillance of bird populations needs to be enhanced to monitor mammalian adaptive mutations of H5N6 viruses.

INTRODUCTION

Influenza viruses are negative-sense, single-stranded, segmented RNA viruses in the *Orthomyxoviridae* family.^{1,2} With reference to two viral surface glycoproteins, hemagglutinin (HA) and neuraminidase (NA), influenza viruses can be divided into 16 HA subtypes (i.e., H1–H16) and 9 NA subtypes (i.e., N1–N9).^{3,4} Beyond that, H17–18 and N10–11 were also recently detected but only in bats.⁵ Although wild waterfowl are reservoirs of influenza viruses, influenza viruses have a broad range of hosts includes poultry, wild birds, pigs, dogs, cats, and humans.^{1,3,4,6,7} Avian influenza H5, H6, H7, and H9 subtype avian influenza viruses were widely prevalence in poultry of China, and at least 9 subtypes of avian influenza viruses have been shown to infect humans, including H5N1, H7N9, H9N2, H5N6, H10N8, H7N4, H10N3, H5N8, and H3N8.^{8,9} Since the first human infection with H5N1 influenza virus in Hong Kong in 1997, H5 subtype influenza viruses have continuously circulated in birds and posed threats to public health.^{10,11} As of August 2022, a total of 865 human infection with H5N1 were reported, with 456 deaths, for a case fatality rate of approximately 53%.¹²

The rapid evolution of H5 subtype viruses has yielded multiple distinct subclades, among which clade 2.3.4.4 now dominates in China.^{13,14} Clade 2.3.4.4 H5Nx influenza viruses were first isolated from poultry in 2008, and have been found to circulate among wild bird and poultry populations ever since.^{13–19} The observation is supported by Bi et al. that H5N6 had replaced H5N1 as the dominant H5 subtype in southern China from 2014 to 2016.¹⁵ Since the first human infections with H5N6 virus was identified in Sichuan Province of China in April 2014, a total of 78 human cases of H5N6 infection (32 deaths) were reported as of August 2022.^{12,20,21} Of recent concern had been the apparent increase in clade 2.3.4.4 H5N6 human infections in China from 2021 to 2022, posing an alarming threat to human health.^{18,21} To manage future outbreaks, the molecular mechanisms by which influenza viruses acquire the ability to infect multiple host species need to be clarified.

The adaptive mutations of influenza viruses are necessary for the efficient virus replication in new host species. Multiple reports have focused on the polymerases of influenza viruses. Polymerases of avian origin generally have impaired activity in human and other mammalian cells.^{22–24} Previous study had

¹Center for Emerging and Zoonotic Diseases, College of Veterinary Medicine, South China Agricultural University, Guangzhou, 510642, China

²National Avian Influenza Para-Reference Laboratory, Guangzhou, 510642, China

³Key Laboratory of Zoonoses, Ministry of Agriculture and Rural Affairs, Guangzhou, 510642, China

⁴National and Regional Joint Engineering Laboratory for Medicament of Zoonoses Prevention and Control, Guangzhou, 510642, China

⁵Key Laboratory of Zoonoses Prevention and Control of Guangdong Province, Guangzhou, 510642, China

⁶These authors contributed equally

⁷Lead contact

*Correspondence: mliao@scau.edu.cn (M.L.), qiwenbao@scau.edu.cn (W.Q.)

<https://doi.org/10.1016/j.isci.2022.105693>



demonstrated that E627K, D701N, and A588V mutations in the PB2 protein increased the virulence of influenza viruses in mammals.^{25–27} Besides, the R195X mutation in the PA-X protein was predominant in human H5N6 viruses and enhanced the adaption of influenza virus in mammals.²⁸ The G622D mutation in the PB1 protein was found to attenuate H5N1 influenza viruses in mice by impairing the binding of PB1 protein to vRNA,²⁹ whereas the S524G mutation of PB1 protein of wild bird-origin H3N8 influenza viruses enhanced the virulence and fitness for transmission in mammals.³⁰

The surface of influenza virion has several crucial components.³¹ The HA protein, for example, is primarily responsible for binding to sialic acid (SA) receptors on the surface of cells.³¹ In addition, four antigenic epitopes on the globular head can target the neutralizing antibodies.^{32,33} Another important surface protein is the NA protein, which plays pivotal roles in the replication and release of virion during the life cycle of influenza virus.³⁴ The NA protein cleaves SA groups from cell glycoproteins, thereby enabling viral release from host cells.³⁵ Other studies also showed that, through the glycan binding, the second receptor binding site (SRBS) of NA can increase the enzymatic activities on multivalent substrates but not monovalent substrates.³⁶ Besides, NA also plays critical role in the virus host adaption and evolution by serving as a receptor-binding protein. For example, the N9 protein of A/tern/Australia/G70C/75(H11N9) alone hemagglutinates animal erythrocytes by using SRBS, that is differ from the NA catalytic site.³⁷ Bao et. al. demonstrated that N-linked glycosylation at 219 position of NA protein is critical to the budding and virulence of influenza viruses.³⁸ Besides, the NA protein of human seasonal H3N2 virus gained a D151G mutation at the NA catalytic site, enabling the viruses to agglutinate erythrocytes in an oseltamivir-sensitive manner.³⁹ Therefore, the adaptive mutation of the NA protein of influenza viruses is also important for the virulence and replication of influenza viruses.

In our study, we found that D272N mutation of the NA protein in H5N6 viruses became predominant in H5N6 viruses since 2015, and that ~85% of human-origin H5N6 viruses harbored amino acid N at position 272 of the NA protein. While examining the replication and virulence of influenza viruses, we found that NA-D272N mutation has enhanced viral replication and the virulence of H5N6 viruses in mice. Our finding firstly provides insights into the function of a mammalian adaptive marker, NA-272, in H5N6 influenza viruses.

RESULTS

Potential mammalian adaptive mutation of D272N is predominant in the NA protein of H5N6 viruses

Current study showed that a sharp increase in the number of human infections with H5N6 influenza viruses occurred in 2021.^{18,40} Knowing that NA protein has numerous functions in the life cycle of influenza viruses, including viral replication and budding,³⁸ we conducted a sequence analysis of NA protein of H5N6 viruses to identify potential mammalian adaptive amino acids. Our results revealed that 272 amino acid residue of NA protein (N6 stalk with no deletion numbering) of H5N6 viruses had undergone a shift from D to N from 2013 to 2021 (Figure 1A). From 2013 to 2014, H5N6 viruses with NA-D272 and NA-N272 were co-circulating in birds and humans; however, since 2015, H5N6 viruses with NA-D272 had dramatically decreased, whereas H5N6 viruses with NA-N272 had become dominant (Figure 1A). We also found that only one human isolate A/Sichuan/26221/2014(H5N6) contained NA-D272 during 2014. From 2015 to 2020, ~85% of the human isolates harbored NA-N272 (see Figure S1), indicative of the dominant NA-272 amino acid residue switch in birds and humans.

D272N mutation in NA protein increased the pathogenicity and replication of H5N6 viruses in mice

To compare the role of 272 amino acid of NA protein in H5N6 viruses, the amino acid N of 272 site in the NA protein of 674 strain was mutated to D by site-directed mutagenesis PCR. Previous study had classified NA genes of H5N6 viruses into two lineages (Major/N6 and Minor/N6), and the NA genes of H5N6 viruses bearing Major/N6 lineage is predominant in China.¹⁵ Therefore, we chose the prevailing H5N6 viruses (A/goose/Guangdong/674/2014) of Major/N6 with NA stalk deletion and assessed the pathogenicity of H5N6 viruses containing amino acid residue 272 D and N of NA protein in mice. Groups of eleven 6-week old female BALB/c mice weighting 14 to 17 g were inoculated intranasally with 10^5 EID₅₀/50 μ L H5N6 viruses. Body weight and percentage of survival of mice in each group were monitored daily for 14 days after infection. All of the mice died when infected with 10^5 EID₅₀/50 μ L H5N6 viruses with 674–272N; however, the mice survived when infected with H5N6 viruses with 674–272D (Figure 1C). The mice infected with 10^5 EID₅₀/50 μ L H5N6 viruses with 674–272N showed significant weight loss after 3

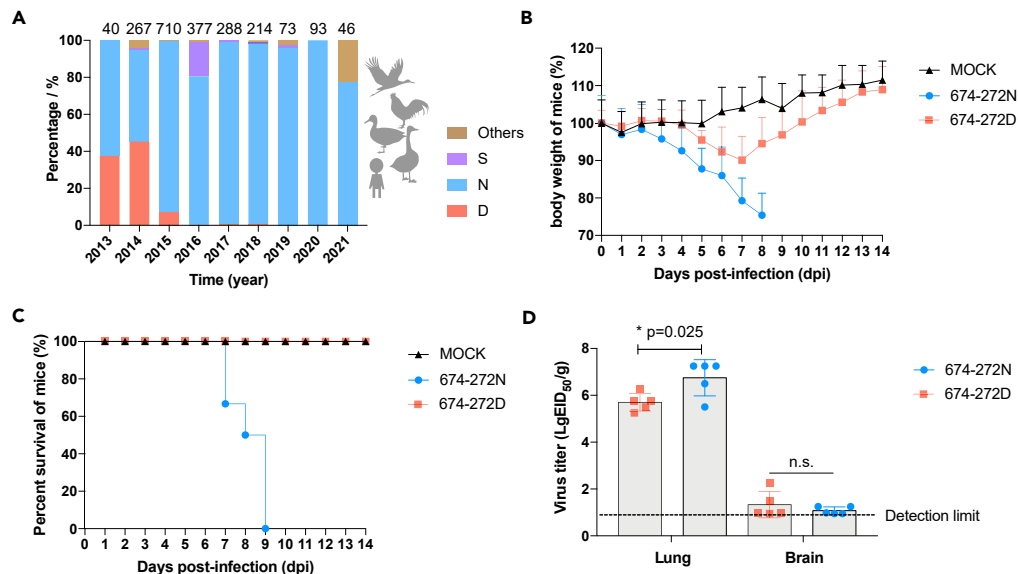


Figure 1. Pathogenicity of H5N6 viruses in mice

(A) Prevalence of amino acid residue 272 in the NA protein of the H5N6 influenza viruses from GISAID's EpiFlu Database from 2013 to 2021. For each column from left to right, the numbers of viruses are 40, 267, 710, 377, 288, 214, 73, 93, and 48, respectively.

(B) Body weight changes of six mice in each group infected with 674–272N and 674–272D viruses in the volume of 10^5 EID₅₀/50 μ L. The values represent the average body weights compared with the baseline weight standard deviations from infected mice.

(C) The percentage of survival rate of the 674–272N and 674–272D viruses.

(D) Five mice infected with 10^5 EID₅₀/50 μ L from each group were euthanized and lung and brain were collected on 4 dpi for virus titration in chicken eggs. Data are represented as means \pm SEM. The independent-samples t-test was used for analysis. The dashed lines indicate the lower limit of detection.

dpi and died within 9 dpi (Figures 1B and 1C), with clear symptoms of infection (e.g., shaggy hair and abdominal breathing). By contrast, the mice infected with H5N6 viruses with 674–272D showed slight weight loss and then rose constantly after 8 dpi (Figure 1B). In addition, five mice in each group were euthanized at 4 dpi and tissue samples, including lung and brain tissue samples, were collected for virus titration via EID₅₀ assay. The results showed that viral titers from 674-272N in mice lungs were significant higher (approximately 1.18-fold, $p = 0.025$) than those of 674–272D (Figure 1D), indicating that H5N6 viruses with NA-272N induce higher replication in mice lung. Besides, no significant differences in the virus titers of mice brains (Figure 1D). These findings suggest that D272N mutation increased the pathogenicity and replication of H5N6 viruses in mice.

D272N mutation in NA protein increased the production and aggressiveness of H5N6 viruses

The multicycle growth kinetics of H5N6 virus with 674–272N and 674–272D were determined for 12, 24, 36, and 48 h in MDCK cells at an MOI of 0.001. In the MDCK cells, the viral replication of 674–272N virus was significantly higher than that of the 674–272D virus at each time point after infection (Figure 2A). We then checked the viral plaque phenotypes of 674–272N and 674–272D by using the standard plaque assay. The plaque diameters of 674–272N were significantly larger (approximately 2.1-fold) than those of 674–272D (Figures 2B–2C). Taken together, those results suggested that D272N mutation in NA protein increased the aggressiveness and the production of H5N6 viruses.

D272N mutation in NA protein increased the thermostability and NA elution ability of H5N6 viruses

To investigate whether D272N mutation in NA protein of H5N6 viruses affects thermostability, we incubated 64 HAU of each virus at 55 $^{\circ}$ C for 5 h and, evaluated the viral titers after every hour of incubation. We found that the titers of 674–272N virus declined over time, but 674–272D virus declined faster and completely lost its infectivity after 1 h of incubation (Figure 2D). These results indicated that the D272N

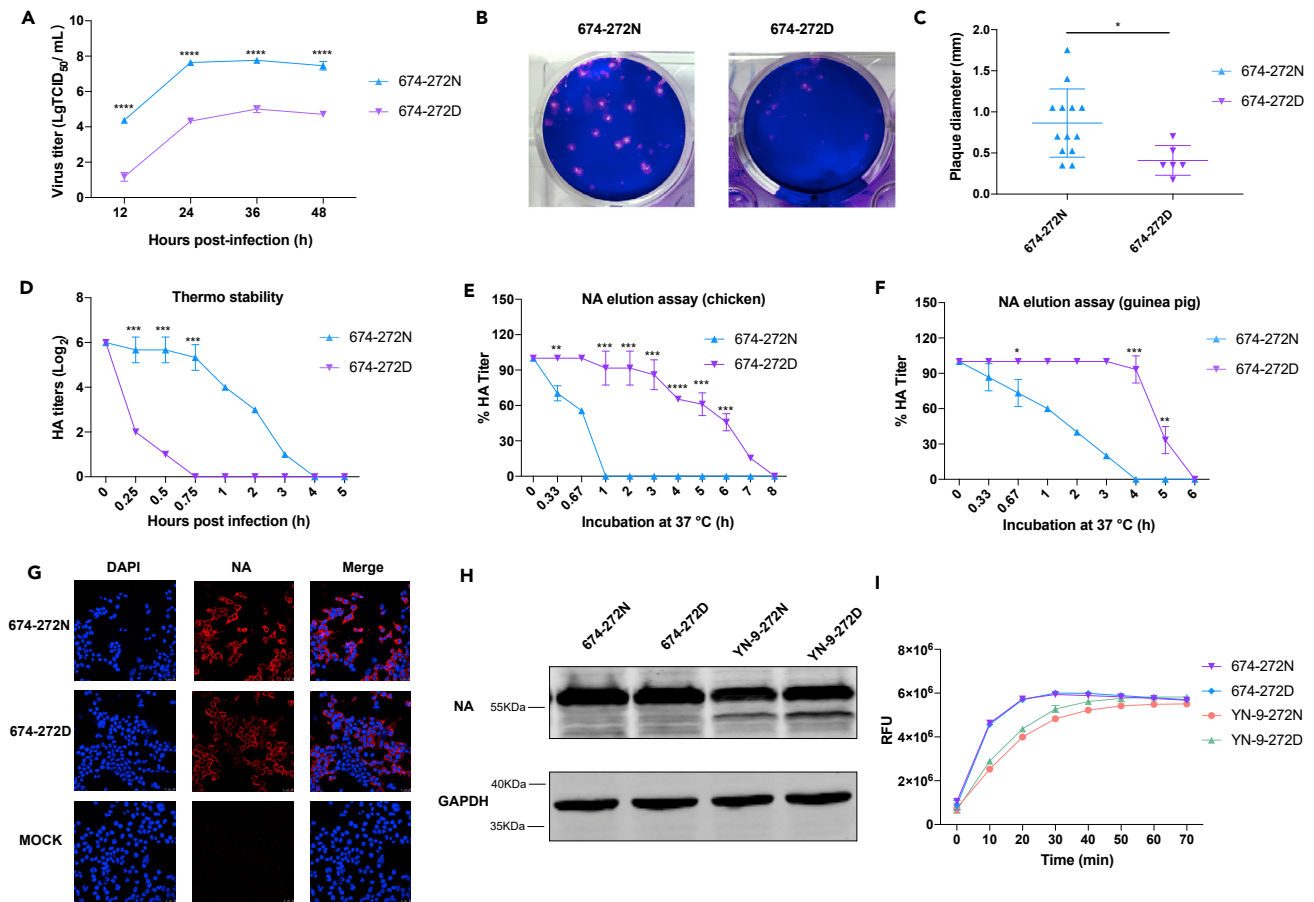


Figure 2. Biological features of H5N6 viruses

(A) Growth curves after inoculation of each virus at a multiplicity of infection (MOI) of 0.001 into MDCK cells. The supernatants of infected cells were collected at the indicated time points. Data are represented as means \pm SEM. The independent-samples t-test was used for analysis.

(B) Plaque-forming ability of the H5N6 viruses in MDCK cell monolayers. Cells were infected with H5N6 virus. After 1 h, cells were washed twice with PBS and then overlaid with MEM containing 1% agarose. After 48 h of incubation, plaques were counted.

(C) Plaque diameters of H5N6 viruses in MDCK cells. Plaque assays were produced under standard conditions and stained with 0.1% crystal violet. The diameters of random plaques were measured for each virus. Data are represented as means \pm SEM. The independent-samples t-test was used for analysis.

(D) Thermostability of the H5N6 viruses. The H5N6 viruses were incubated for 15 min, 30 min, 45 min, 1 h, 2 h, 3 h, 4 h, and 5 h at 55°C. The titers of heat-treated H5N6 viruses were determined by HA assay. Data are represented as means \pm SEM. The independent-samples t-test was used for analysis.

(E) NA elution assay results in chicken erythrocytes. Different H5N6 viruses were adsorbed to a 1% suspension of chicken at 4°C for 30 min, and the HA titers at 37°C representing virus elution from guinea pig erythrocytes was monitored each hour for 8 h. The HA titers following incubation at 37°C is expressed as the percentage of the HA titers at time zero at 4°C. Data are represented as means \pm SEM. The independent-samples t-test was used for analysis.

(F) NA elution assay results in guinea pig erythrocytes. Different H5N6 viruses were adsorbed to a 1% suspension of guinea pig erythrocytes at 4°C for 30 min, and the HA titers at 37°C representing virus elution from guinea pig erythrocytes was monitored each hour for 8 h. The HA titers following incubation at 37°C is expressed as the percentage of the HA titers at time zero at 4°C. Data are represented as means \pm SEM. The independent-samples t-test was used for analysis.

(G) The HEK293T cells were transfected with corresponding plasmids for 24 h. NA proteins were localized by immunofluorescence (red). Nuclei were stained with DAPI (blue).

(H) Protein levels of the NA protein of transfected 293T cells. 293T cells were transfected with plasmids expressing wild-type NA (674–272N and YN-9-272N) and a NA mutant (674–272D and YN-9-272D).

(I) NA enzymatic activity of different NAs of H5N6 viruses. HEK293T cell monolayers were transfected with each plasmid. The samples were analyzed using an NA assay kit according to the manufacturer's instructions.

mutation in NA protein increased thermal stability of H5N6 influenza viruses. Previous studies showed that NA affected the release of viruses bound to erythrocytes; thus, elution of H5N6 viruses with different NA-272 amino acid residues from erythrocytes was compared. Briefly, H5N6 viruses were adsorbed on chicken and guinea pig erythrocytes at 4°C for 30 min, and release at 37°C was monitored for 8 h. Elution of the 674–272N viruses from chicken and guinea pig erythrocytes were complete after 1 h and 4 h of

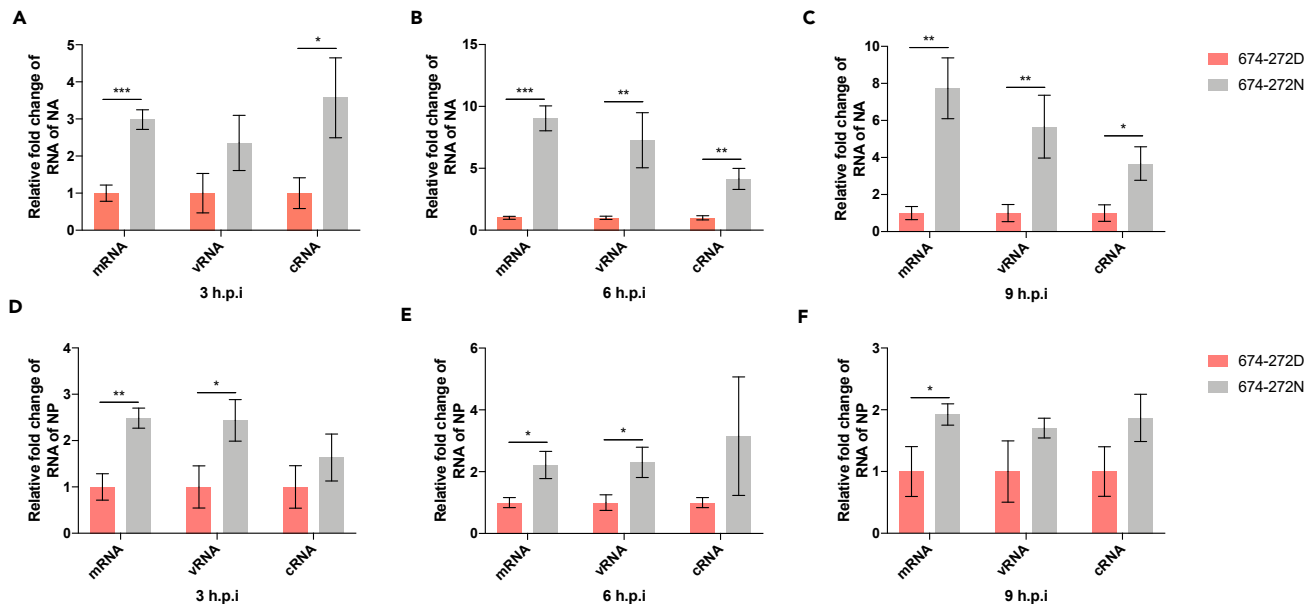


Figure 3. Transcription of the NA and NP proteins of H5N6 viruses

(A) Relative expression levels of viral NA mRNAs, vRNAs, and cRNAs of the 674–272D and 674–272N viruses in MDCK cells. MDCK cells were infected with the indicated H5N6 viruses at an MOI of 1 for 3 h. mRNAs, vRNAs, and cRNAs expression levels of NA genes in MDCK cells are presented as fold changes relative to the values for the 674–272D virus.

(B) Relative expression levels of viral NA mRNAs, vRNAs, and cRNAs of the 674–272D and 674–272N viruses in MDCK cells. MDCK cells were infected with the indicated H5N6 viruses at an MOI of 1 for 6 h. mRNAs, vRNAs, and cRNAs expression levels of NA genes in MDCK cells are presented as fold changes relative to the values for the 674–272D virus.

(C) Relative expression levels of viral NA mRNAs, vRNAs, and cRNAs of the 674–272D and 674–272N viruses in MDCK cells. MDCK cells were infected with the indicated H5N6 viruses at an MOI of 1 for 9 h. mRNAs, vRNAs, and cRNAs expression levels of NA genes in MDCK cells are presented as fold changes relative to the values for the 674–272D virus.

(D) Relative expression levels of viral NP mRNAs, vRNAs, and cRNAs of the 674–272D and 674–272N viruses in MDCK cells. MDCK cells were infected with the indicated H5N6 viruses at an MOI of 1 for 3 h. mRNAs, vRNAs, and cRNAs expression levels of NP genes in MDCK cells are presented as fold changes relative to the values for the 674–272D virus.

(E) Relative expression levels of viral NP mRNAs, vRNAs, and cRNAs of the 674–272D and 674–272N viruses in MDCK cells. MDCK cells were infected with the indicated H5N6 viruses at an MOI of 1 for 6 h. mRNAs, vRNAs, and cRNAs expression levels of NP genes in MDCK cells are presented as fold changes relative to the values for the 674–272D virus.

(F) Relative expression levels of viral NP mRNAs, vRNAs, and cRNAs of the 674–272D and 674–272N viruses in MDCK cells. MDCK cells were infected with the indicated H5N6 viruses at an MOI of 1 for 9 h. mRNAs, vRNAs, and cRNAs expression levels of NP genes in MDCK cells are presented as fold changes relative to the values for the 674–272D virus. Data are represented as means \pm SEM. Statistical significance was indicated as * ($p < 0.05$), ** ($p < 0.01$), and *** ($p < 0.001$). The independent-samples t-test was used for analysis.

incubation, respectively (Figures 2E and 2F). In contrast, the 674–272D viruses were only partially eluted from chicken and guinea pig erythrocytes after 1 h and 4 h, respectively, and were completely eluted from chicken and guinea pig erythrocytes after 8 h and 6 h of incubation, respectively (Figures 2E and 2F). Taken together, our results showed the evidence that 674–D272N increased the thermostability and NA elution of H5N6 viruses from erythrocytes.

D272N mutation in NA protein did not affect NA enzymatic activity

To compare the expression of NA protein of 674–272N and 674–272D, HEK293T cell monolayers were transfected with pPRE-674-272N-Flag and pPRE-674-272D-Flag plasmids, and the WB and IFA results showed that no significant differences were observed in NA protein of N272 and D272 (Figures 2G and 2H). To explore whether D272N mutation affected the NA enzymatic activity, the NA enzymatic activity of the NA protein of N272 and mutant D272 was tested. The result indicated that D272N mutation did not affect the NA enzymatic activity (Figure 2I). In addition, we also assessed the NA enzymatic activity of prevailing H5N6 viruses isolated from 2016 (A/duck/Yunnan/YN-9/2016(H5N6)) bearing the amino acids D272 and N272. The result suggested that no significant differences were found in the expression of NA

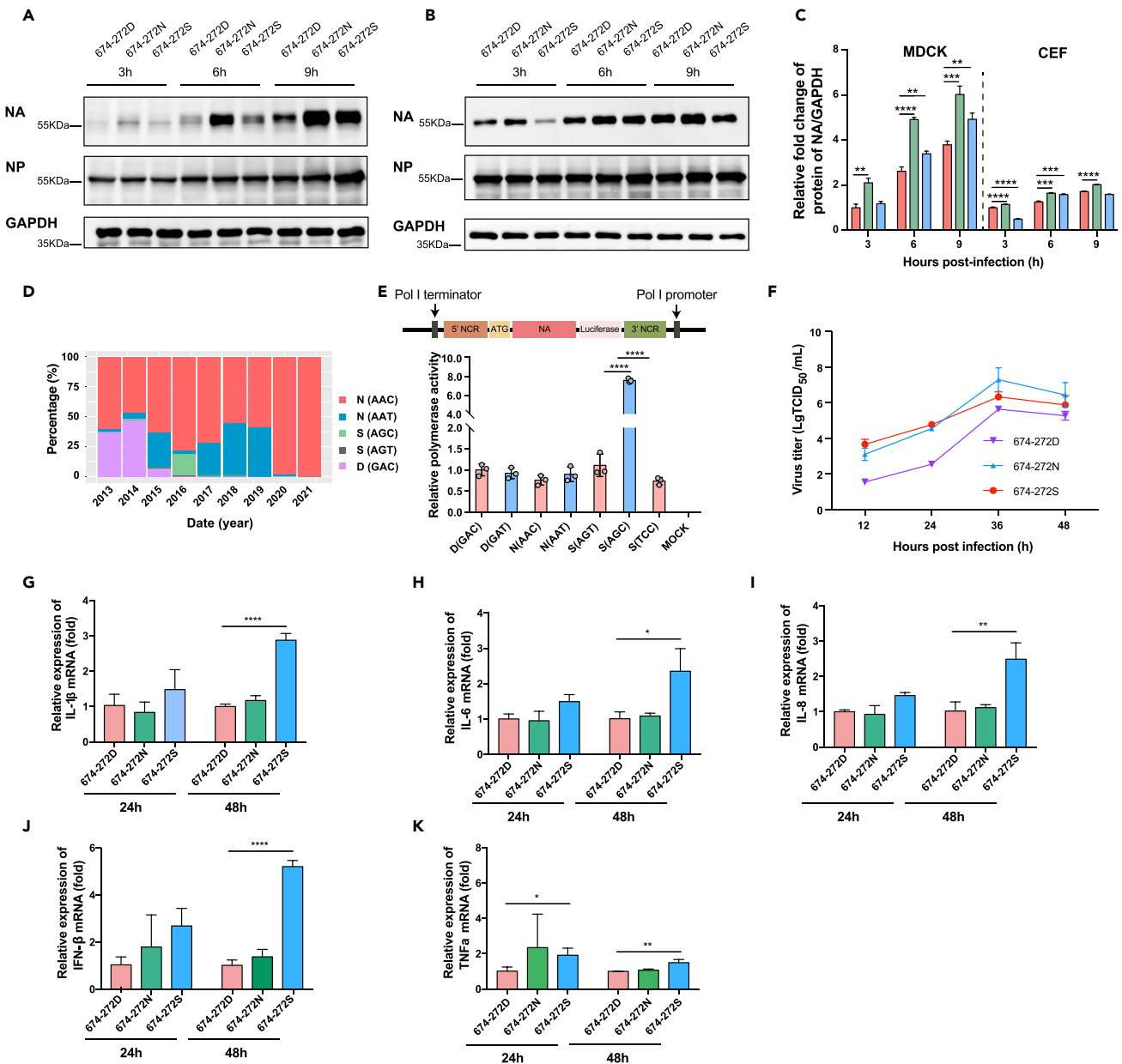


Figure 4. Expression of the NA protein and detection of the mRNA levels of the inflammatory cytokines of H5N6 viruses

(A) Western blots of cell cultures from MDCK cell cultures inoculated with H5N6 viruses at an MOI of 1 for 3, 6, and 9 h. Virus protein was detected with specific antibodies against NA and NP.

(B) Western blots of cell cultures from CEF cell cultures inoculated with H5N6 viruses at an MOI of 1 for 3, 6, and 9 h. Virus protein was detected with specific antibodies against NA and NP.

(C) Grayscale analysis of NA proteins of the H5N6 viruses infected with MDCK and CEF cells. Relative NA protein expression were calculated according to the equation NA/GAPDH. Data are represented as means \pm SEM. The independent-samples t-test was used for analysis. Statistical significance was indicated as * ($p < 0.05$), ** ($p < 0.01$), *** ($p < 0.001$), **** ($p < 0.0001$).

(D) Prevalence of the codon of amino acid residue 272 in the NA protein of H5N6 influenza viruses from GISAID's EpiFlu Database from 2013 to 2021.

(E) The reporter plasmids were constructed by inserting different NA whose sequences were derived from those opening reading frame (ORF) of NA gene in 674 strain between a start codon and the remaining ORF of the firefly luciferase gene. 293T cells were transfected with different NA plasmids, including NA gene sequences contained amino acid D (GAC and GAT codon), N (AAC and AAT codon), S (AGT, AGC, and TCC codon). Luciferase production was assayed using the dual-luciferase reporter assay system (Promega) according to the manufacturer's instructions. Each point on the curve is the mean \pm standard deviation from three independent experiments. The independent-samples t-test was used for analysis. Data are represented as means \pm SEM. The independent-samples t-test was used for analysis. Statistical significance was indicated as * ($p < 0.05$), ** ($p < 0.01$), *** ($p < 0.001$), **** ($p < 0.0001$).

(F) Growth curves after the inoculation of each virus into MDCK cells. The supernatants of infected cells were collected at the indicated time points.

Figure 4. Continued

(G) A549 cells were infected with different H5N6 viruses as indicated. After 24 and 48 h, total RNA was extracted for qPCR analyses with the indicated primers. Relative expression of mRNA level of IL-1 β were indicated. The mRNA expression levels of IL-1 β was expressed as fold changes in relation to the 674–272D. (H) A549 cells were infected with different H5N6 viruses as indicated. After 24 and 48 h, total RNA was extracted for qPCR analyses with the indicated primers. Relative expression of mRNA level of IL-6 were indicated. The mRNA expression levels of IL-6 was expressed as fold changes in relation to the 674–272D. (I) A549 cells were infected with different H5N6 viruses as indicated. After 24 and 48 h, total RNA was extracted for qPCR analyses with the indicated primers. Relative expression of mRNA level of IL-8 were indicated. The mRNA expression levels of IL-8 was expressed as fold changes in relation to the 674–272D. (J) A549 cells were infected with different H5N6 viruses as indicated. After 24 and 48 h, total RNA was extracted for qPCR analyses with the indicated primers. Relative expression of mRNA level of IFN- β were indicated. The mRNA expression levels of IFN- β was expressed as fold changes in relation to the 674–272D. (K) A549 cells were infected with different H5N6 viruses as indicated. After 24 and 48 h, total RNA was extracted for qPCR analyses with the indicated primers. Relative expression of mRNA level of TNF- α were indicated. The mRNA expression levels of TNF- α was expressed as fold changes in relation to the 674–272D. Data are represented as means \pm SEM. The independent-samples t-test was used for analysis. Statistical significance was indicated as * ($p < 0.05$), ** ($p < 0.01$), *** ($p < 0.001$), **** ($p < 0.0001$).

protein bearing N272 and D272, and D272N mutation did not affect the NA enzymatic activity (Figures 2H and 2I).

D272N mutation in NA protein increased viral transcription, genomic replication, and expression of NA protein

The performance of viral RNP polymerase in viral transcription (mRNA), cRNA, and genomic replication (vRNA) was evaluated in MDCK cells with 674–272N and 674–272D viruses at 3, 6, and 9 hpi. qRT-PCR analysis with mRNA, vRNA, and cRNA-specific primers indicated that 674–272N produced significantly higher levels of NA mRNA, vRNA, and cRNA at 3, 6, and 9 dpi (Figures 3A–3C); however, significant differences of NP mRNA and vRNA were observed in 674–272D and 674–272N viruses (Figures 3D–3F). These results suggested that D272N mutation increased the viral NA and NP transcription and replication in MDCK cells.

We next examined the viral protein expression in MDCK cells separately infected with the 674–272N and 674–272D viruses at 3, 6, and 9 hpi. At each time point, the NA protein expression of 674–272N virus produced higher levels of the NA protein than the 674–272D virus did, whereas no significant differences of NP protein expression were observed between the 674–272N and 674–272D viruses (Figures 4A and 4C). We then examined the viral protein expression in avian CEF cells separately infected with the 674–272N and 674–272D viruses at 3, 6, and 9 hpi. Our findings also suggested that the NA protein expression of 674–272N virus produced higher levels of the NA protein than the 674–272D, whereas no significant differences of NP protein expression were observed between the 674–272N and 674–272D viruses (Figures 4B and 4C); however, the fold-change of the NA protein between 674–272D and 674–272N in CEF cells was significantly lower than that of in MDCK cells (Figures 4A–4C). Taken together, the accumulation of the NA protein was earlier and greater during infection with the 674–272N virus than with the corresponding 674–272D virus.

N272S mutation in NA protein in wild bird-origin H5N6 viruses increased the transcription of the NA protein but did not increase the viral replication

We found that the dominant 272 residue switch from N to S occurred in wild bird-origin H5N6 viruses since late 2016 (see Figure S1). To evaluate whether N272S mutation has influenced viral replication, the amino acid residue 272 of the NA protein was mutated to S, and the mutant virus was designated 674–272S. We found no significant difference in viral replication in the MDCK cells between the 674–272N and 674–272S viruses. We next examined viral protein expression in MDCK and CEF cells separately infected with the 674–272S viruses at 3, 6, and 9 hpi. The expression of the NA and NP protein of the 674–272N virus produced higher levels of the protein than the 674–272S virus did at each time point; however, in the latter stage, no significant difference in the expression of NP protein was observed between the 674–272N and 674–272S viruses (Figures 4A–4C).

To evaluate whether RNA secondary structure influence the transcription of NA protein in different amino acid motif of 272 residues, a reporter assay was established to detect the NA expression in the RNA sequences encoding the amino acids of NA protein. In our reporter plasmids, the firefly luciferase gene lacking its start codon was inserted downstream of the start codon, and the firefly luciferase was expressed when nucleotides were inserted into the NA protein to make the sequence in frame with the open reading frame. The synonymous mutation of amino acid D, N, and S of 272 residues of NA gene were conducted, designating D (GAC), D (GAT), N (AAC), N (AAT), S (AGT), S (AGC), and S (TCC). Our results showed that no significant differences of luciferase expression were observed between D (GAC), D (GAT), N (AAC), and N

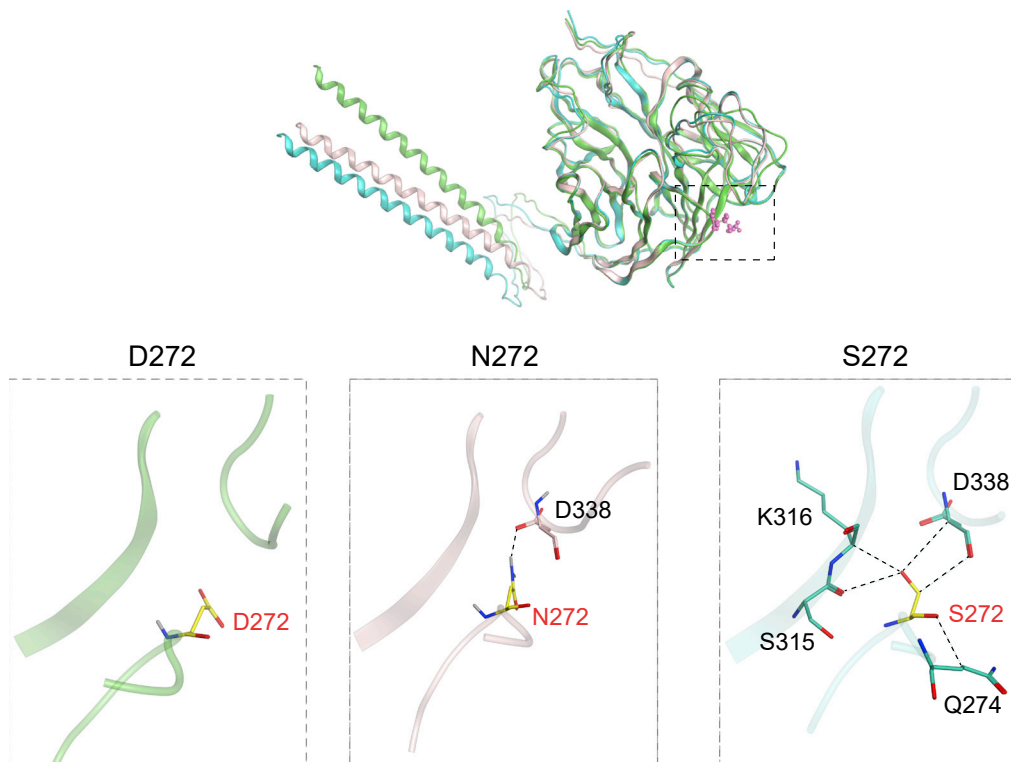


Figure 5. Three-dimensional (3D) structure analysis of amino acids at 272 site in the NA protein

Each NA protein of 674–272D, 674–272N, and 674–272S had five stimulated models ranked by pLDDT. The structural similarity RMSD and pLDDT ranking were taken into consideration to choose the final model. The final three best-fit models of each group were used in the following analysis. The corresponding amino acids to a 3D structure of the NA protein containing different amino acid motifs were mapped using Pymol (<https://pymol.org/2/support.html/>).

(AAT). However, the S (AGC) significantly enhanced the luciferase expression compared with S (AGT) and S (TCC) (Figure 4E). These findings suggested the amino acid S of 272 residue with different codon motifs affected the NA protein expression of H5N6 viruses.

N272S mutation in NA protein of wild bird-origin H5N6 viruses induced an elevated proinflammatory response in human cells

Several viral infections of influenza in humans and animal models are associated with abnormally elevated pulmonary expression levels of proinflammatory cytokines such as TNF- α , IFN- β , IL-1 β , IL-6, and IL-8. To compare the proinflammatory impacts of 674–272D, 674–272N, and 674–272S viruses, we determined the mRNA expression levels of the cytokines in A549 cells infected with the 674–272D, 674–272N, and 674–272S viruses at 24 and 48 hpi. No significant differences in the mRNA expression levels of the five cytokines were observed in A549 cells infected with the 674–272D and 674–272N viruses at 24 and 48 hpi (Figures 4G–4K). Although no significant differences in viral replication in the MDCK cells were observed in either virus (Figure 4F), the 674–272S virus induced higher levels of mRNA expression of TNF- α , IFN- β , IL-1 β , IL-6, and IL-8 at 48 hpi than the 674–272N virus did (Figures 4G–4K). Taken together, our results suggest that N272S mutation significantly increased the expression levels of proinflammatory cytokines in infected A549 cells.

Structure analysis of amino acid residue 272 in NA protein of H5N6 viruses

Each NA protein of 674–272D, 674–272N, and 674–272S had five stimulated models ranked by predicted local distance difference test (pLDDT).⁴¹ The structural similarity root-mean-square deviation (RMSD) and pLDDT ranking were taken into consideration to choose the final model. Compared with amino acid D272, we found that the elongated side chain of amino acid N272 made it have the closer distance to amino acid D327 to cause molecular interaction (Figure 5). Of interest, compared with amino acids D272 and

N272, amino acid S272 might have more interactions with surrounding amino acid residues (K316, S315, D338, and Q274) (Figure 5). These findings suggested that the structure of NA protein with amino acid D272 might be unstable compared with NA protein with amino acids N272 and S272.

DISCUSSION

Highly pathogenic H5N6 avian influenza viruses are endemic in poultry and wild bird populations in China.^{14,42} It is noteworthy that it had crossed the barrier to infect humans.¹⁴ Although H5N6 infection in humans have been reported sporadically in China since 2014, a spike in the number of human infections with the viruses was reported in 2021^{20,21}, and outbreaks of H5N6 viruses have also frequently occurred in poultry and wild bird populations. For those reasons, H5N6 viruses have become a major concern for not only poultry farming and wildlife security but also public health.⁴³ Therefore, the molecular mechanisms by which influenza viruses acquire the ability to infect humans urgently need to be clarified. In our study, we found that an amino acid substitution in the NA protein plays a key role in the virulence of H5N6 viruses in mice and in their replication in mammalian cells. Further sequence analysis demonstrated that the D272N mutation in the NA protein has become predominant in H5N6 viruses since 2015. In particular, ~85% of human isolates bear amino acid N at position 272, thereby indicating that the D272N mutation at the NA protein of H5N6 viruses is increasing in prevalence.

Successful replication and virulence in a new host is a chief requirement for the cross-species transmission of avian influenza viruses, which may rely on the reassortment and multiple adaptive mutations.^{44–47} A well-known E627K mutation in the PB2 protein is of remarkable host-associated genetic significance, for it increases virulence in mice, guinea pigs, and ferrets and can cause severe disease resulting from human infection.^{25,48–52} Although the polymerase of influenza viruses is critical for their cross-species transmission, the surface genes of the viruses are also important in the entry and release of the viruses. Gu et al. showed that the combination of HA2-N154D and NA-V202I could influence the viral biological properties *in vivo* and *in vitro*.⁵³ In our study, another molecular risk marker of H5N6 viruses, namely the 272 position of the NA protein was also identified. We found that the D272N mutation in the NA protein of H5N6 viruses significantly increased virulence in mice by increasing replication in mammalian cells, early transcription, and the accumulation of NA proteins in mammalian cells. There is also epidemiological evidence of avian viruses with mutations, akin to D272N mutation of NA protein of H5N6, that confer mammalian tropism and have emerged or become predominant in avian strains before transmission to mammals.

Similar to D272N mutation of NA protein, 226 and 228 sites of the HA protein are important for the receptor binding ability and virulence in mice.^{54,55} Wang et al. have also shown that the introduction of N-linked glycosylation (NLG) site at position 158–160 of HA protein of H5N1 viruses enhanced viral productivity in infected mammalian cells and exacerbates host immune response to viral infection.⁵⁶ However, in our study, the D272N mutation of NA protein did not increase the expression levels of proinflammatory cytokines in infected A549 cells, thereby indicating that the D272N mutation of NA protein did not exacerbate host immune and inflammatory response to viral infection. We also found that D272N mutation of NA protein increased the viral thermostability and release of the viruses from erythrocytes. Recent studies have also demonstrated that the NLG site at position 219 of NA protein plays an important role in the budding, replication, and virulence of H1N1 influenza viruses.³⁸ In our study, 14 NLG sites of NA protein in 674 strains were identified, and we found that NA-272 is not NLG site, indicating that minor function of NLG play a role in shaping the phenotype of this key mutation. However, we generated evidence that the D272N mutation in the NA protein of H5N6 viruses significantly increases virulence in mice by increasing replication in mammalian cells, early transcription and the accumulation of NA protein in mammalian cells, suggestive of the minor influence of the budding of the NA protein. Past studies have also shown that the mutation of the HA or NA protein of influenza viruses could stack in endoplasmic reticulum (ER) for refolding or be destroyed through ER-associated degradation.^{38,57} However, in our study, we did not detect any influence of ER-stress genes induced by D272N mutation of NA protein (data not shown), which suggests that different genetic changes in the NA protein of influenza viruses alter pathogenicity via different molecular mechanisms.

Given the long-distance migration of wild birds, the innate capacity for reassortment and genetic mutations of influenza viruses, and their increased human-type receptor-binding capability, the global spread and potential zoonotic risk of H5N6 viruses to humans should not be ignored. Therefore, the amino acid residue 272 of the NA protein of wild bird-origin H5N6 viruses was also analyzed. We found that the

dominant 272 residue switch from N to S has occurred in wild bird-origin H5N6 viruses since late 2016. To evaluate whether N272S mutation influences viral replication, we mutated the amino acid residue 272 of the NA protein to S (i.e., 674–272S). Although no significant difference in viral replication was observed between the 674–272N and 674–272S viruses in mammalian cells, we found that the 674–272S virus induced higher levels of the expression of proinflammatory cytokines in infected A549 cells than the 674–272D and 674–272N viruses did, thereby indicating that amino acid residue S in position 272 of wild bird-origin H5N6 viruses poses an elevated risk to humans. Previous studies had demonstrated that NA genes of H5N6 viruses were originated from H6N6.^{15,58} We also analyzed the proportion of amino acid motifs of NA-272 in H6N6 viruses. We found that the dominant amino acid motif of NA-272 is N (see [Figure S2](#)), which is consistent with that of H5N6 viruses. The structures of RNA molecules were important for the RNA-editing mechanism. In our study, amino acid S of 272 residue with different codons affected the expression of NA protein in H5N6 viruses, and the codon AGC of NA-272 significantly enhanced the NA protein expression of H5N6 viruses, and we also found that the dominant codon AGC of NA-272 occurred in H5N6 viruses ([Figure 4D](#)), which suggests that the underlying RNA secondary structure might have been affected and thus requires further investigation. Structural analysis demonstrated amino acid residue S in position 272 of wild bird-origin H5N6 viruses acquired four additional direct links with amino acids K316, S315, D338, and Q274, thereby indicating that the structure of NA protein with amino acid S272 might be more stable compared with NA protein with amino acids D272.

In sum, we found that the D272N mutation in the NA protein of H5N6 viruses has become dominant in birds and humans. D272N mutation in the NA protein plays a key role in increasing the virulence of H5N6 viruses in mice by increasing replication in mammalian cells, thermostability, released virus from erythrocytes, early transcription, and the accumulation of NA protein in mammalian cells. We identified a mammalian adaptive marker in the NA protein of H5N6 influenza viruses, which offer insights into the new target for the development for the attenuated vaccines and antiviral drugs. Considering the sharp increase in the number of human infections with H5N6 viruses, the surveillance of poultry and wild bird populations needs to be enhanced to monitor mammalian adaptive mutations of H5N6 viruses and to gauge the potential threat posed to humans.

Limitations of the study

In this study, we identified a risk marker in the NA protein of highly pathogenic influenza A H5N6 virus. We found that D272N mutation in the NA protein plays a key role in increasing the virulence of H5N6 viruses in mice. Recent study showed that evidence that compared to individuals exposed to cases of H7N9 viruses, a significantly higher probability of infection was observed in the individuals exposed to H5N1 viruses.⁵⁹ Therefore, the transmission model like ferret is also critical to assess in the future. In addition, other studies had showed that the combined mutations can influence the pathogenicity and replication of influenza viruses. Therefore, the spectrum of mutations together with NA-D272N should also be taken into consideration.

STAR★METHODS

Detailed methods are provided in the online version of this paper and include the following:

- [KEY RESOURCES TABLE](#)
- [RESOURCE AVAILABILITY](#)
 - Lead contact
 - Materials availability
 - Data and code availability
- [METHODS DETAILS](#)
 - Ethics statement and biosafety
- [EXPERIMENTAL MODEL AND SUBJECT DETAILS](#)
 - Virus isolation and cells
 - Amino acid analysis of NA-272 of H5N6 viruses
 - Plasmid construction and reverse genetics
 - Replication and virulence of H5N6 viruses in mice
 - Virus growth kinetics
 - Western blotting
 - Virus plaque assay

- Hemagglutination–elution assay
- Thermostability assay
- Construction and eukaryotic expression of plasmids
- Neuraminidase activity assay
- Indirect immunofluorescent assay
- Luciferase reporter assay
- Quantitative real-time PCR (qRT-PCR)
- Select the appropriate model of NA protein stimulated by ColabFold and structure superposition and comparison

- **QUANTIFICATION AND STATISTICAL ANALYSIS**

SUPPLEMENTAL INFORMATION

Supplemental information can be found online at <https://doi.org/10.1016/j.isci.2022.105693>.

ACKNOWLEDGMENTS

We acknowledge the authors, originating and submitting laboratories of the sequences from GISAID's EpiFlu Database on which this research is based. All submitters of data may be contacted directly through the GISAID website (www.gisaid.org). This work was supported by the Guangdong Major Project of Basic and Applied Basic Research (2020B0301030007), National Natural Science Foundation of China (31830097 and 31672586), the Key Research and Development Program of Guangdong Province (2019B020218004), Earmarked Found for China Agriculture Research System (CARS-41-G16), Guangdong Province Universities and Colleges Pearl River Scholar Funded Scheme (2018, Wenbao Qi), and Young Scholars of Yangtze River Scholar Professor Program (2019, Wenbao Qi).

AUTHOR CONTRIBUTIONS

J.H.Z., X.M.W., M.L., and W.B.Q. conceived and designed the experiment. J.H.Z., K.X.M., Y.G., T.Z., and Y.L. performed *in vivo* experiment. J.H.Z., X.M.W., S.P.D., and Y.T.J. performed *in vitro* experiment. J.H.Z., H.N.L., and W.B.Q. contributed analysis. J.H.Z., M.L., and W.B.Q. draft the manuscript. All authors reviewed and revised the first and final drafts of this manuscript. M.L. and W.B.Q. are co-corresponding authors who contributed equally to this article.

DECLARATION OF INTERESTS

The authors declare no competing interests.

Received: July 29, 2022

Revised: October 14, 2022

Accepted: November 24, 2022

Published: December 22, 2022

REFERENCES

1. Webster, R.G., Bean, W.J., Gorman, O.T., Chambers, T.M., and Kawaoka, Y. (1992). Evolution and ecology of influenza A viruses. *Microbiol. Rev.* 56, 152–179. <https://doi.org/10.1128/mr.56.1.152-179.1992>.
2. Yoon, S.W., Webby, R.J., and Webster, R.G. (2014). Evolution and ecology of influenza A viruses. *Curr. Top. Microbiol. Immunol.* 385, 359–375. https://doi.org/10.1007/82_2014_396.
3. Su, S., Bi, Y., Wong, G., Gray, G.C., Gao, G.F., and Li, S. (2015). Epidemiology, evolution, and recent outbreaks of avian influenza virus in China. *J. Virol.* 89, 8671–8676. <https://doi.org/10.1128/JVI.01034-15>.
4. Su, S., Gu, M., Liu, D., Cui, J., Gao, G.F., Zhou, J., and Liu, X. (2017). Epidemiology, evolution, and pathogenesis of H7N9 influenza viruses in five epidemic waves since 2013 in China. *Trends Microbiol.* 25, 713–728. <https://doi.org/10.1016/j.tim.2017.06.008>.
5. Wu, Y., Wu, Y., Tefsen, B., Shi, Y., and Gao, G.F. (2014). Bat-derived influenza-like viruses H17N10 and H18N11. *Trends Microbiol.* 22, 183–191. <https://doi.org/10.1016/j.tim.2014.01.010>.
6. Su, S., Xing, G., Wang, J., Li, Z., Gu, J., Yan, L., Lei, J., Ji, S., Hu, B., Gray, G.C., et al. (2016). Characterization of H7N2 avian influenza virus in wild birds and pikas in qinghai-tibet plateau area. *Sci. Rep.* 6, 30974. <https://doi.org/10.1038/srep30974>.
7. Zhou, J., Sun, W., Wang, J., Guo, J., Yin, W., Wu, N., Li, L., Yan, Y., Liao, M., Huang, Y., et al. (2009). Characterization of the H5N1 highly pathogenic avian influenza virus derived from wild pikas in China. *J. Virol.* 83, 8957–8964. <https://doi.org/10.1128/JVI.00793-09>.
8. Liu, W.J., Wu, Y., Bi, Y., Shi, W., Wang, D., Shi, Y., and Gao, G.F. (2022). Emerging HxNy influenza A viruses. *Cold Spring Harb. Perspect. Med.* 12, a038406. <https://doi.org/10.1101/cshperspect.a038406>.
9. Yang, R., Sun, H., Gao, F., Luo, K., Huang, Z., Tong, Q., Song, H., Han, Q., Liu, J., Lan, Y., et al. (2022). Human infection of avian influenza A H3N8 virus and the viral origins: a descriptive study. *Lancet. Microbe* 3, e824–e834. <https://doi.org/10.1016/S2666-5247>.

10. Guan, Y., Shortridge, K.F., Krauss, S., and Webster, R.G. (1999). Molecular characterization of H9N2 influenza viruses: were they the donors of the "internal" genes of H5N1 viruses in Hong Kong? *Proc. Natl. Acad. Sci. USA* 96, 9363–9367. <https://doi.org/10.1073/pnas.96.16.9363>.
11. Xu, X., Subbarao, Cox, N.J., and Guo, Y. (1999). Genetic characterization of the pathogenic influenza A/Goose/Guangdong/1/96 (H5N1) virus: similarity of its hemagglutinin gene to those of H5N1 viruses from the 1997 outbreaks in Hong Kong. *Virology* 261, 15–19. <https://doi.org/10.1006/viro.1999.9820>.
12. Zhang, L., Liu, K., Su, Q., Chen, X., Wang, X., Li, Q., Wang, W., Mao, X., Xu, J., Zhou, X., et al. (2022). Clinical features of the first critical case of acute encephalitis caused by avian influenza A (H5N6) virus. *Emerg. Microb. Infect.* 11, 2437–2446. <https://doi.org/10.1080/22221751.2022.2122584>.
13. Yamaji, R., Saad, M.D., Davis, C.T., Swayne, D.E., Wang, D., Wong, F.Y.K., McCauley, J.W., Peiris, J.S.M., Webby, R.J., Fouchier, R.A.M., et al. (2020). Pandemic potential of highly pathogenic avian influenza clade 2.3.4.4 A(H5) viruses. *Rev. Med. Virol.* 30, e2099. <https://doi.org/10.1002/rmv.2099>.
14. Zhang, J., Chen, Y., Shan, N., Wang, X., Lin, S., Ma, K., Li, B., Li, H., Liao, M., and Qi, W. (2020). Genetic diversity, phylogeography, and evolutionary dynamics of highly pathogenic avian influenza A (H5N6) viruses. *Virus Evol.* 6, veaa079. <https://doi.org/10.1093/ve/veaa079>.
15. Bi, Y., Chen, Q., Wang, Q., Chen, J., Jin, T., Wong, G., Quan, C., Liu, J., Wu, J., Yin, R., et al. (2016). Genesis, evolution and prevalence of H5N6 avian influenza viruses in China. *Cell Host Microbe* 20, 810–821. <https://doi.org/10.1016/j.chom.2016.10.022>.
16. Bi, Y., Liu, H., Xiong, C., Di, L., Shi, W., Li, M., Liu, S., Chen, J., Chen, G., Li, Y., et al. (2016). Novel avian influenza A (H5N6) viruses isolated in migratory waterfowl before the first human case reported in China, 2014. *Sci. Rep.* 6, 29888. <https://doi.org/10.1038/srep29888>.
17. Gu, M., Liu, W., Cao, Y., Peng, D., Wang, X., Wan, H., Zhao, G., Xu, Q., Zhang, W., Song, Q., et al. (2011). Novel reassortant highly pathogenic avian influenza (H5N5) viruses in domestic ducks, China. *Emerg. Infect. Dis.* 17, 1060–1063. <https://doi.org/10.3201/eid1706.101406>.
18. Zhang, J., Ye, H., Liu, Y., Liao, M., and Qi, W. (2022). Resurgence of H5N6 avian influenza virus in 2021 poses new threat to public health. *Lancet. Microbe* 3, e558. <https://doi.org/10.1016/S2666-5247>.
19. Zhang, J., Li, X., Wang, X., Ye, H., Li, B., Chen, Y., Chen, J., Zhang, T., Qiu, Z., Li, H., et al. (2021). Genomic evolution, transmission dynamics, and pathogenicity of avian influenza A (H5N8) viruses emerging in China, 2020. *Virus Evol.* 7, veab046. <https://doi.org/10.1093/ve/veab046>.
20. Pan, M., Gao, R., Lv, Q., Huang, S., Zhou, Z., Yang, L., Li, X., Zhao, X., Zou, X., Tong, W., et al. (2016). Human infection with a novel, highly pathogenic avian influenza A (H5N6) virus: virological and clinical findings. *J. Infect.* 72, 52–59. <https://doi.org/10.1016/j.jinf.2015.06.009>.
21. Wille, M., and Barr, I.G. (2022). Resurgence of avian influenza virus. *Science* 376, 459–460. <https://doi.org/10.1126/science.abo1232>.
22. Labadie, K., Dos Santos Afonso, E., Rameix-Welti, M.A., van der Werf, S., and Naffakh, N. (2007). Host-range determinants on the PB2 protein of influenza A viruses control the interaction between the viral polymerase and nucleoprotein in human cells. *Virology* 362, 271–282. <https://doi.org/10.1016/j.virol.2006.12.027>.
23. Mehle, A., and Doudna, J.A. (2009). Adaptive strategies of the influenza virus polymerase for replication in humans. *Proc. Natl. Acad. Sci. USA* 106, 21312–21316. <https://doi.org/10.1073/pnas.0911915106>.
24. Rameix-Welti, M.A., Tomoiu, A., Dos Santos Afonso, E., van der Werf, S., and Naffakh, N. (2009). Avian Influenza A virus polymerase association with nucleoprotein, but not polymerase assembly, is impaired in human cells during the course of infection. *J. Virol.* 83, 1320–1331. <https://doi.org/10.1128/JVI.00977-08>.
25. Hatta, M., Gao, P., Halfmann, P., and Kawakami, Y. (2001). Molecular basis for high virulence of Hong Kong H5N1 influenza A viruses. *Science* 293, 1840–1842. <https://doi.org/10.1126/science.1062882>.
26. Li, Z., Chen, H., Jiao, P., Deng, G., Tian, G., Li, Y., Hoffmann, E., Webster, R.G., Matsuoka, Y., and Yu, K. (2005). Molecular basis of replication of duck H5N1 influenza viruses in a mammalian mouse model. *J. Virol.* 79, 12058–12064. <https://doi.org/10.1128/JVI.79.18.12058-12064.2005>.
27. Xiao, C., Ma, W., Sun, N., Huang, L., Li, Y., Zeng, Z., Wen, Y., Zhang, Z., Li, H., Li, Q., et al. (2016). PB2-588 V promotes the mammalian adaptation of H10N8, H7N9 and H9N2 avian influenza viruses. *Sci. Rep.* 6, 19474. <https://doi.org/10.1038/srep19474>.
28. Sun, Y., Hu, Z., Zhang, X., Chen, M., Wang, Z., Xu, G., Bi, Y., Tong, Q., Wang, M., Sun, H., et al. (2020). An R195K mutation in the PA-X protein increases the virulence and transmission of influenza A virus in mammalian hosts. *J. Virol.* 94, e01817–e01819. <https://doi.org/10.1128/JVI.01817-19>.
29. Feng, X., Wang, Z., Shi, J., Deng, G., Kong, H., Tao, S., Li, C., Liu, L., Guan, Y., and Chen, H. (2016). Glycine at position 622 in PB1 contributes to the virulence of H5N1 avian influenza virus in mice. *J. Virol.* 90, 1872–1879. <https://doi.org/10.1128/JVI.02387-15>.
30. Zhang, X., Li, Y., Jin, S., Zhang, Y., Sun, L., Hu, X., Zhao, M., Li, F., Wang, T., Sun, W., et al. (2021). PB1 S524G mutation of wild bird-origin H3N8 influenza A virus enhances virulence and fitness for transmission in mammals. *Emerg. Microb. Infect.* 10, 1038–1051. <https://doi.org/10.1080/22221751.2021.1912644>.
31. Kosik, I., and Yewdell, J.W. (2019). Influenza hemagglutinin and neuraminidase: Yin(-) Yang proteins coevolving to thwart immunity. *Viruses* 11. <https://doi.org/10.3390/v11040346>.
32. Wu, N.C., and Wilson, I.A. (2020). Influenza hemagglutinin structures and antibody recognition. *Cold Spring Harb. Perspect. Med.* 10, a038778. <https://doi.org/10.1101/cshperspect.a038778>.
33. Russell, C.J., Hu, M., and Okda, F.A. (2018). Influenza hemagglutinin protein stability, activation, and pandemic risk. *Trends Microbiol.* 26, 841–853. <https://doi.org/10.1016/j.tim.2018.03.005>.
34. McAuley, J.L., Gilbertson, B.P., Trifkovic, S., Brown, L.E., and McKimm-Breschkin, J.L. (2019). Influenza virus neuraminidase structure and functions. *Front. Microbiol.* 10, 39. <https://doi.org/10.3389/fmicb.2019.00039>.
35. Wen, F., and Wan, X.F. (2019). Influenza neuraminidase: underrated role in receptor binding. *Trends Microbiol.* 27, 477–479. <https://doi.org/10.1016/j.tim.2019.03.001>.
36. Uhlenhorff, J., Matrosovich, T., Klenk, H.D., and Matrosovich, M. (2009). Functional significance of the hemadsorption activity of influenza virus neuraminidase and its alteration in pandemic viruses. *Arch. Virol.* 154, 945–957. <https://doi.org/10.1007/s00705-009-0393-x>.
37. Webster, R.G., Air, G.M., Metzger, D.W., Colman, P.M., Varghese, J.N., Baker, A.T., and Laver, W.G. (1987). Antigenic structure and variation in an influenza virus N9 neuraminidase. *J. Virol.* 61, 2910–2916. <https://doi.org/10.1128/JVI.61.9.2910-2916.1987>.
38. Bao, D., Xue, R., Zhang, M., Lu, C., Ma, T., Ren, C., Zhang, T., Yang, J., Teng, Q., Li, X., et al. (2021). N-linked glycosylation plays an important role in budding of neuraminidase protein and virulence of influenza viruses. *J. Virol.* 95, 020422–e2120. <https://doi.org/10.1128/JVI.02042-20>.
39. Zhu, X., McBride, R., Nycholat, C.M., Yu, W., Paulson, J.C., and Wilson, I.A. (2012). Influenza virus neuraminidases with reduced enzymatic activity that avidly bind sialic acid receptors. *J. Virol.* 86, 13371–13383. <https://doi.org/10.1128/JVI.01426-12>.
40. Zhu, W., Li, X., Dong, J., Bo, H., Liu, J., Yang, J., Zhang, Y., Wei, H., Huang, W., Zhao, X., et al. (2022). Epidemiologic, clinical, and genetic characteristics of human infections with influenza A(H5N6) viruses, China. *Emerg. Infect. Dis.* 28, 1332–1344. <https://doi.org/10.3201/eid2807.212482>.
41. Mirdita, M., Schütze, K., Moriawaki, Y., Heo, L., Ovchinnikov, S., and Steinegger, M. (2022). ColabFold: making protein folding accessible to all. *Nat. Methods* 19, 679–682. <https://doi.org/10.1038/s41592-022-01488-1>.
42. Zhang, J., Lao, G., Zhang, R., Wei, Z., Wang, H., Su, G., Shan, N., Li, B., Li, H., Yu, Y., et al. (2018). Genetic diversity and dissemination pathways of highly pathogenic H5N6 avian influenza viruses from birds in Southwestern

- China along the East Asian-Australian migration flyway. *J. Infect.* 76, 418–422. <https://doi.org/10.1016/j.jinf.2017.11.009>.
43. Shi, W., and Gao, G.F. (2021). Emerging H5N8 avian influenza viruses. *Science* 372, 784–786. <https://doi.org/10.1126/science.abg6302>.
 44. de Wit, E., Munster, V.J., van Riel, D., Beyer, W.E.P., Rimmelzwaan, G.F., Kuiken, T., Osterhaus, A.D.M.E., and Fouchier, R.A.M. (2010). Molecular determinants of adaptation of highly pathogenic avian influenza H7N7 viruses to efficient replication in the human host. *J. Virol.* 84, 1597–1606. <https://doi.org/10.1128/JVI.01783-09>.
 45. Lloren, K.K.S., Lee, T., Kwon, J.J., and Song, M.S. (2017). Molecular markers for interspecies transmission of avian influenza viruses in mammalian hosts. *Int. J. Mol. Sci.* 18, 2706. <https://doi.org/10.3390/ijms18122706>.
 46. Zanin, M., Wong, S.S., Barman, S., Kaewborisuth, C., Vogel, P., Rubrum, A., Darnell, D., Marinova-Petkova, A., Krauss, S., Webby, R.J., and Webster, R.G. (2017). Molecular basis of mammalian transmissibility of avian H1N1 influenza viruses and their pandemic potential. *Proc. Natl. Acad. Sci. USA* 114, 11217–11222. <https://doi.org/10.1073/pnas.1713974114>.
 47. Li, F., Liu, J., Yang, J., Sun, H., Jiang, Z., Wang, C., Zhang, X., Yu, Y., Zhao, C., Pu, J., et al. (2021). H9N2 virus-derived M1 protein promotes H5N6 virus release in mammalian cells: mechanism of avian influenza virus interspecies infection in humans. *PLoS Pathog.* 17, e1010098. <https://doi.org/10.1371/journal.ppat.1010098>.
 48. Gao, P., Watanabe, S., Ito, T., Goto, H., Wells, K., McGregor, M., Cooley, A.J., and Kawaoka, Y. (1999). Biological heterogeneity, including systemic replication in mice, of H5N1 influenza A virus isolates from humans in Hong Kong. *J. Virol.* 73, 3184–3189. <https://doi.org/10.1128/JVI.73.4.3184-3189.1999>.
 49. Govorkova, E.A., Rehg, J.E., Krauss, S., Yen, H.L., Guan, Y., Peiris, M., Nguyen, T.D., Hanh, T.H., Puthavathana, P., Long, H.T., et al. (2005). Lethality to ferrets of H5N1 influenza viruses isolated from humans and poultry in 2004. *J. Virol.* 79, 2191–2198. <https://doi.org/10.1128/JVI.79.4.2191-2198.2005>.
 50. Steel, J., Lowen, A.C., Mubareka, S., and Palese, P. (2009). Transmission of influenza virus in a mammalian host is increased by PB2 amino acids 627K or 627E/701N. *PLoS Pathog.* 5, e1000252. <https://doi.org/10.1371/journal.ppat.1000252>.
 51. de Jong, M.D., Simmons, C.P., Thanh, T.T., Hien, V.M., Smith, G.J.D., Chau, T.N.B., Hoang, D.M., Chau, N.V.V., Khanh, T.H., Dong, V.C., et al. (2006). Fatal outcome of human influenza A (H5N1) is associated with high viral load and hypercytokinemia. *Nat. Med.* 12, 1203–1207. <https://doi.org/10.1038/nm1477>.
 52. Fouchier, R.A.M., Schneeberger, P.M., Rozendaal, F.W., Broekman, J.M., Kemink, S.A.G., Munster, V., Kuiken, T., Rimmelzwaan, G.F., Schutten, M., Van Doornum, G.J.J., et al. (2004). Avian influenza A virus (H7N7) associated with human conjunctivitis and a fatal case of acute respiratory distress syndrome. *Proc. Natl. Acad. Sci. USA* 101, 1356–1361. <https://doi.org/10.1073/pnas.0308352100>.
 53. Gu, M., Zhao, Y., Ge, Z., Li, Y., Gao, R., Wang, X., Hu, J., Liu, X., Hu, S., Peng, D., and Liu, X. (2022). Effects of HA2 154 deglycosylation and NA V202I mutation on biological property of H5N6 subtype avian influenza virus. *Vet. Microbiol.* 266, 109353. <https://doi.org/10.1016/j.vetmic.2022.109353>.
 54. Wan, H., and Perez, D.R. (2007). Amino acid 226 in the hemagglutinin of H9N2 influenza viruses determines cell tropism and replication in human airway epithelial cells. *J. Virol.* 81, 5181–5191. <https://doi.org/10.1128/JVI.02827-06>.
 55. DuBois, R.M., Zaraket, H., Reddivari, M., Heath, R.J., White, S.W., and Russell, C.J. (2011). Acid stability of the hemagglutinin protein regulates H5N1 influenza virus pathogenicity. *PLoS Pathog.* 7, e1002398. <https://doi.org/10.1371/journal.ppat.1002398>.
 56. Wang, W., Lu, B., Zhou, H., Suguitan, A.L., Jr., Cheng, X., Subbarao, K., Kemple, G., and Jin, H. (2010). Glycosylation at 158N of the hemagglutinin protein and receptor binding specificity synergistically affect the antigenicity and immunogenicity of a live attenuated H5N1 A/Vietnam/1203/2004 vaccine virus in ferrets. *J. Virol.* 84, 6570–6577. <https://doi.org/10.1128/JVI.00221-10>.
 57. Yin, Y., Yu, S., Sun, Y., Qin, T., Chen, S., Ding, C., Peng, D., and Liu, X. (2020). Glycosylation deletion of hemagglutinin head in the H5 subtype avian influenza virus enhances its virulence in mammals by inducing endoplasmic reticulum stress. *Transbound. Emerg. Dis.* 67, 1492–1506. <https://doi.org/10.1111/tbed.13481>.
 58. Yang, L., Zhu, W., Li, X., Bo, H., Zhang, Y., Zou, S., Gao, R., Dong, J., Zhao, X., Chen, W., et al. (2017). Genesis and dissemination of highly pathogenic H5N6 avian influenza viruses. *J. Virol.* 91, 021999–e2216. <https://doi.org/10.1128/JVI.02199-16>.
 59. Chen, X., Wang, W., Qin, Y., Zou, J., and Yu, H. (2022). Global epidemiology of human infections with variant influenza viruses, 1959–2021: a descriptive study. *Clinical Infectious Diseases* (an official publication of the Infectious Diseases Society of America). <https://doi.org/10.1093/cid/ciac168>.
 60. Katoh, K., Misawa, K., Kuma, K.I., and Miyata, T. (2002). MAFFT: a novel method for rapid multiple sequence alignment based on fast Fourier transform. *Nucleic Acids Res.* 30, 3059–3066. <https://doi.org/10.1093/nar/gkf436>.
 61. Hoffmann, E., Neumann, G., Kawaoka, Y., Hobom, G., and Webster, R.G. (2000). A DNA transfection system for generation of influenza A virus from eight plasmids. *Proc. Natl. Acad. Sci. USA* 97, 6108–6113. <https://doi.org/10.1073/pnas.100133697>.
 62. Hoffmann, E., Stech, J., Guan, Y., Webster, R.G., and Perez, D.R. (2001). Universal primer set for the full-length amplification of all influenza A viruses. *Arch. Virol.* 146, 2275–2289. <https://doi.org/10.1007/s007050170002>.
 63. Yu, Y., Zhang, Z., Li, H., Wang, X., Li, B., Ren, X., Zeng, Z., Zhang, X., Liu, S., Hu, P., et al. (2017). Biological characterizations of H5Nx avian influenza viruses embodying different neuraminidases. *Front. Microbiol.* 8, 1084. <https://doi.org/10.3389/fmicb.2017.01084>.
 64. Wang, X., Zeng, Z., Zhang, Z., Zheng, Y., Li, B., Su, G., Li, H., Huang, L., Qi, W., and Liao, M. (2018). The appropriate combination of hemagglutinin and neuraminidase prompts the predominant H5N6 highly pathogenic avian influenza virus in birds. *Front. Microbiol.* 9, 1088. <https://doi.org/10.3389/fmicb.2018.01088>.
 65. Sun, Y., Tan, Y., Wei, K., Sun, H., Shi, Y., Pu, J., Yang, H., Gao, G.F., Yin, Y., Feng, W., et al. (2013). Amino acid 316 of hemagglutinin and the neuraminidase stalk length influence virulence of H9N2 influenza virus in chickens and mice. *J. Virol.* 87, 2963–2968. <https://doi.org/10.1128/JVI.02688-12>.
 66. Qian, G., Wang, S., Chi, X., Li, H., Wei, H., Zhu, X., Chen, Y., and Chen, J.L. (2014). The amino-terminal region of the neuraminidase protein from avian H5N1 influenza virus is important for its biosynthetic transport to the host cell surface. *Vet. J.* 202, 612–617. <https://doi.org/10.1016/j.tvjl.2014.10.015>.

STAR★METHODS

KEY RESOURCES TABLE

REAGENT or RESOURCE	SOURCE	IDENTIFIER
<i>Antibody</i>		
Anti-GAPDH	TransGen Biotech	Cat#HC301-01
Anti-Flag	Sigma	Cat#F3165
Anti-Influenza A virus NP	Sino Biological	Cat#11657-MM03T
Anti-Influenza A virus NA	Sino Biological	Cat#40235-RP01-100
HRP	Jackson	Lot No. 135756
Secondary antibody Mouse	LI-COR	Lot#D20125-35
Secondary antibody Rabbit	LI-COR	Lot#D20208-05
<i>Chemicals, peptides and recombinant proteins</i>		
DAPI	GENVIEW	CAT#GD3410-10ML
TPCK-Trypsin	GIBCO	Lot#2488393
10x loading	Vazyme	L/N 017E2212AA
DNA ladder	Vazyme	L/N 027E2232CA
Protein ladder	Vazyme	Lot# 91246561
SuperKine™ Enhanced Antibody Dilution Buffer	Abbkine	CAT#BMU103-CN
Western Blot Fast Stripping Buffer	Shanghai Epizyme Biomedical Technology Co., Ltd	CAT#PS107
XhoI	NEW ENGLAND BioLabs	Cat#R0146L
NotI	NEW ENGLAND BioLabs	Cat#R0189L
Bsmbl-v2	NEW ENGLAND BioLabs	Cat#R0739L
DMEM	GIBCO	Lot#91246561
BSA	VWR	Lot#21E2456215
TPCK	Sigma	Cat#T1426-250MG
PBS	Biosharp	Cat#BL601A
TBS	Beijing Dingguo Changsheng Biotechnology Co., Ltd	Cat#BF-0153
Triton X-100	Beijing Dingguo Changsheng Biotechnology Co., Ltd	Cat#DH351-4
Carbinol	GENERAL-REAGENT	Lot#P2059864
Paraformaldehyde	Biosharp	Lot#70110900
Agrose	TSINGKE	Cat#TSJ001
Opti-MEM	GIBCO	Cat#11058021
2XMEM	GIBCO	Cat#61100061
Lipofectamine 2000	Invitrogen	Cat#11668019
<i>Critical commercial assays</i>		
Dual-Luciferase Reporter Assay System	Promega	E1910
RNAfast200	Shanghai Feijie Co., Ltd	Cat#220011
Gel Extraction Kit D2500	OMEGA	Cat#D2500-02
HiScript II 1st Strand cDNA Synthesis Kit	Vazyme	L/N 7E562J1
Green Taq Mix	Vazyme	L/N B2242AAB
2×Phanta Max Master Mix	Vazyme	L/N 7E530K1

(Continued on next page)

Continued

REAGENT or RESOURCE	SOURCE	IDENTIFIER
2xSYBR PCR master mix	Vazyme	L/N 027E2201CC
Neuraminidase Assay Kit	Beyotime	Cat#P0306
Experimental models: Cell lines		
HEK293T	In-house	N/A
A549	In-house	N/A
CEF	In-house	N/A
MDCK	In-house	N/A
Experimental models: Strain		
A/goose/Guangdong/SH7/2013 (H5N1)	N/A	EPL_ISL_259927
A/goose/Guangdong/674/2014 (H5N6)	N/A	EPL_ISL_259924
Experimental models: Mouse		
BALB/c mice	Vital River Company	N/A
Oligonucleotides		
Forward primer of 674–272D-F1 for site-directed mutagenesis PCR TATTGGTCTCAGGGAGCAAAGCAGGAGT	This paper	N/A
Forward primer of 674–272D-F2 for site-directed mutagenesis PCR TGAAGAAGTCAAGGGGACGCTCAAC	This paper	N/A
Reverse primer of 674–272D-R1 for site-directed mutagenesis PCR GTTGAGCGTCCCCTTGCAAGTTCTTCA	This paper	N/A
Reverse primer of 674–272D-R2 for site-directed mutagenesis PCR ATATGGTCTCGTATTAGTAGAAACAA GGAGTTTTTT	This paper	N/A
Forward primer of 674–272S-F1 for site-directed mutagenesis PCR TATTGGTCTCAGGGAGCAAAGCA GGAGT	This paper	N/A
Forward primer of 674–272S-F2 for site-directed mutagenesis PCR CTGCAAGGGAGTGCTCAACACATCG AAGAGTGT	This paper	N/A
Reverse primer of 674–272S-R1 for site-directed mutagenesis PCR TCGATGTGTTGAGCACTCCCTTGAG TTCTCAA	This paper	N/A
Reverse primer of 674–272S-R1 for site-directed mutagenesis PCR ATATGGTCTCGTATTAGTAGAAACAAG GAGTTTTTT	This paper	N/A
The strand-specific primer sequences for NA mRNA CCAGATCGTTCGAGTCGTTTTTTTTTT TTTTTCTTAAACT ATTTCTAC	This paper	N/A
The strand-specific primer sequences for NA cRNA GCTAGCTTCAGCTAGGCATCtAGTAGA AACAAGG AGTTTTTCTTA	This paper	N/A

(Continued on next page)

Continued

REAGENT or RESOURCE	SOURCE	IDENTIFIER
The strand-specific primer sequences for NA vRNA GGCCGTCATGGTGCGAATAAAGGAATCT GC CCAGTGGTCATG	This paper	N/A
The strand-specific primer sequences for NP mRNA CCAGATCGTTCGAGTCGTTTTTTTTTTTTTTT TTCTTTAATTGTCATACT	This paper	N/A
The strand-specific primer sequences for NP cRNA GCTAGCTTCAGCTAGGCATCAGTAG AAACAAGGGTATT	This paper	N/A
The strand-specific primer sequences for NP vRNA GGCCGTCATGGTGCGAATTAACGAC CGGAATTTCTGGAGAGG	This paper	N/A
Forward primer of NA mRNA TCCAATAGCATGGT AGCTCTCTGT	This paper	N/A
Forward primer of NA cRNA TCCAATAGCATGGTAGCTCTCTGT	This paper	N/A
Forward primer of NA vRNA GGCCGTCATGGTGCGAAT	This paper	N/A
Forward primer of NP mRNA TCGGACGAAAAGGCAACGAA	This paper	N/A
Forward primer of NP cRNA TCGGACGAAAAGG CAACGAA	This paper	N/A
Forward primer of NP vRNA GGCCGTCATGGTGCGAAT	This paper	N/A
Reverse primer of NA mRNA CCAGATCGTTCGAGTCGT	This paper	N/A
Reverse primer of NA cRNA TCCAATAGCATGGTAGCTCTCTGT	This paper	N/A
Reverse primer of NA vRNA GGCCGTCATGGTGCGAAT	This paper	N/A
Reverse primer of NP mRNA CCAGATCGTTCGAGTCGT	This paper	N/A
Reverse primer of NP cRNA GCTAGCTTCAGCTAGGCATC	This paper	N/A
Reverse primer of NP vRNA CAGCATTCCCAGGATTTCTGCTC	This paper	N/A
Forward primer of IL-1 β GCTGATGGCCCTAAACAGATGA	This paper	N/A
Forward primer of IL-6 AAGCCAGAGCTGTGCAGATGAGTA	This paper	N/A
Forward primer of IL-8 TTTCAGAGACAGCAGAGCACA	This paper	N/A
Forward primer of TNF- α CTCAGCAAGGACAGCAGAGG	This paper	N/A
Forward primer of IFN- β AGGACAGGATGAACTTTGAC	This paper	N/A
Reverse primer of IL-1 β TCCATGGCCACAACAAGTGC	This paper	N/A
Reverse primer of IL-6 TGCCTGCAGCCACTGGTTC	This paper	N/A

(Continued on next page)

Continued

REAGENT or RESOURCE	SOURCE	IDENTIFIER
Reverse primer of IL-8 CACACAGAGCTGCAGAAATCAG	This paper	N/A
Reverse primer of TNF- α ATGTGGCGTCTGAGGGTTGTT	This paper	N/A
Reverse primer of IFN- β TGATAGACATTAGCCAGGA	This paper	N/A
Forward primer of GAPDH (canine) TGGAGAAAGCTGCCAAATAT	This paper	N/A
Reverse primer of GAPDH (canine) TGGGTGTCAGTGTGAAGT	This paper	N/A
Recombinant DNA		
pRRE-674-272D	This paper	N/A
pRRE-674-272N	This paper	N/A
pRRE-YN-9-272D	This paper	N/A
pRRE-YN-9-272N	This paper	N/A
PHW2000-SH7-PB2	This paper	N/A
PHW2000-SH7-PB1	This paper	N/A
PHW2000-SH7-PA	This paper	N/A
PHW2000-SH7-NP	This paper	N/A
PHW2000-SH7-M	This paper	N/A
PHW2000-SH7-NS	This paper	N/A
PHW2000-674-NA-272D	This paper	N/A
PHW2000-674-NA-272N	This paper	N/A
PHW2000-674-NA-272S	This paper	N/A
Software and algorithms		
GraphPad Prism 7.0	Dotmatics	N/A
ImageJ	National Institutes of Health	N/A
SnapGene	Dotmatics	N/A
MAFFT v 7.313 program	60	N/A
pLDDT	41	N/A
Pymol	DeLano Scientific LLC	N/A
Others		
Chicken erythrocytes	South China Agricultural University	N/A
Guinea pig erythrocytes	Guangzhou Ruite Biotechnology Co., Ltd	N/A

RESOURCE AVAILABILITY**Lead contact**

Further information and requests for resources and reagents should be directed to and will be fulfilled by the lead contact, Wenbao Qi (qiwenbao@scau.edu.cn).

Materials availability

All unique constructs generated in this study are available from the [lead contact](#).

Data and code availability

- All data reported in this paper will be shared by the [lead contact](#) upon request.
- This paper does not report an original code.

- Any additional information required to reanalyze the data reported in this paper is available from the [lead contact](#) upon request.

METHODS DETAILS

Ethics statement and biosafety

All experiments with all available influenza A (H5N6) viruses were conducted in an animal biosafety level 3 laboratory and animal facility following South China Agricultural University (SCAU) (CNAS BL0011) protocols. All animals involved in experiments were reviewed and approved by the Institution Animal Care and Use Committee at SCAU and treated in accordance with the guidelines (2017A002).

EXPERIMENTAL MODEL AND SUBJECT DETAILS

All of the animals in this study were 6-week-old female BALB/c mice weighting 14 to 17 g, obtained from the Vital River Company in Beijing. We provided sufficient feed and water for experimental animals every day.

Virus isolation and cells

The viruses used, namely the H5N1 viruses A/goose/Guangdong/SH7/2013 (H5N1) (SH7; accession number: EPI_ISL_259927) and the H5N6 virus A/goose/Guangdong/674/2014 (H5N6) (674; accession number: EPI_ISL_259924), were isolated from sick geese. All viruses were propagated in 10-day-old SPF embryonated eggs at 37 °C and frozen at –80 °C. All cells used, including human embryonic kidney (HEK293T) cells, MDCK cells, and A549 cells were provided by the National Avian Influenza Para-Reference Laboratory (Guangzhou) at South China Agricultural University. HEK293T, MDCK, and A549 cells were grown in Dulbecco's modified Eagle's medium supplemented with 10% calf serum, 100 U/mL penicillin, and 0.1 mg/mL streptomycin and incubated at 37 °C in a 5% CO₂ incubator.

Amino acid analysis of NA-272 of H5N6 viruses

All available NA genome sequences with the complete coding regions of H5N6 viruses were downloaded from GISAID (<http://www.gisaid.org/>), and were aligned using MAFFT v 7.313 program.⁶⁰ The number of each amino acid motifs of 272 site were analyzed using Python 3.10 and visualized using R 4.1.3.

Plasmid construction and reverse genetics

The internal gene segments from the SH7 strain were cloned into Hoffmann's bidirectional transcription vector pHW2000 plasmid system,^{61,62} as were the HA and NA genes of the 674 strain. We reasoned that the insertion of the internal genes of SH7 and the surface genes of 674 strain cDNAs between a pol I promoter and a pol II promoter should result in the transcription of eight vRNAs, all viral mRNAs, and in the synthesis of at least 10 proteins.⁶¹ The amino acid N of 272 site in the NA gene of the 674 strain was mutated to D and S by site-directed mutagenesis PCR. The primers used for site-directed mutagenesis PCR were available from [key resources table](#). The recombination H5N6 viruses carrying the HA and NA genes of the 674 strain with internal gene segments of the SH7 were generated using reverse genetics. The H5N6 viruses bearing amino acids D, N, and S in 272 site of NA protein were labeled "674–272D", "674–272N", and "674–272S", respectively. Briefly, HEK293T cell monolayers in 12-well plates were transfected at 80–90% confluency with 2.4 μg of the eight plasmids (300 ng of each plasmid) using Lipofectamine 2000 (Invitrogen) according to the manufacturer's instructions. DNA and transfection reagent were mixed and incubated at room temperature for 20 min and added to the cells. Four hours later, the mixture was replaced with Opti-MEM (GIBCO) containing 0.2% bovine serum albumin. After 48 hours, the supernatant was harvested and injected into SPF embryonated eggs for virus propagation. The H5N6 viruses were confirmed by RT-PCR and sequencing.

Replication and virulence of H5N6 viruses in mice

Groups of eleven 6-week-old female BALB/c mice weighting 14 to 17 g, obtained from the Vital River Company in Beijing, were anesthetized with isoflurane and inoculated intranasally with 10⁵ EID₅₀ of H5N6 viruses in a volume of 50 μL. Body weight and clinical signs of six mice were monitored daily for 14 day post-infection (dpi), and mice were euthanized if they lost more than 25% of their initial body weight. To test for virus replication in the organs, five mice in each group were euthanized at 4 dpi and tissue samples, including lung and brain tissue samples, were collected for virus titration by an EID₅₀ assay.

Virus growth kinetics

Confluent MDCK cells were infected with 674–272N and 674–272D viruses at a multiplicity of infection (MOI) of 0.001 TCID₅₀/cell for 1 h at 37 °C. After 1 h of incubation, the cells were washed twice with phosphate-buffered saline (PBS), and incubated with DMEM containing 0.2% bovine serum albumin (BSA; Dingguo, Beijing, China) at 37°C with 5% CO₂. Culture supernatants were collected at the indicated time points (12 hpi, 24 hpi, 36 hpi, and 48 hpi) and stored at –80°C until use. Viral titres were determined via TCID₅₀ assay in the MDCK cells.

Western blotting

The MDCK and CEF cells were inoculated with the H5N6 viruses at an MOI of 1 in the absence of TPCK-trypsin for 3, 6, and 9 h in minimal essential medium containing 0.2% BSA (Dingguo, Beijing, China). Proteins from the cell cultures were separated on 8% sodium dodecyl sulfate–polyacrylamide gel electrophoresis (SDS–PAGE) gels and then electrotransferred onto nitrocellulose membranes. Polyclonal rabbit anti-NA antibody from the H4N6 virus A/mallard/Ohio/657/2002 (H4N6) (1:1,000 dilution for 2 h at room temperature; Sino Biological Inc., Beijing, China) was used to detect NA; polyclonal mouse anti-NP antibody from influenza A nucleoprotein/NP antibody (1:1000 dilution for 2 h at room temperature; Sino Biological Inc., Beijing, China) was used to detect NP; and monoclonal mouse anti-GAPDH (HC301, Transgen) was used to detect GAPDH. Goat anti-rabbit or mouse IgG conjugated with horseradish peroxidase (1:10,000 dilution for 30 min at room temperature; Dingguo, Beijing, China) was used as a secondary antibody, followed by chemiluminescence detection the Odyssey Imaging System (LI-COR). A grayscale analysis of individual bands was performed using ImageJ v1.45.

Virus plaque assay

The plaque assay was adapted from previously described procedure.^{63,64} After MDCK cells were grown in DMEM and seeded onto 12-well plates, confluent monolayers were washed twice with PBS and infected with serial 10-fold dilutions of the virus at 37 °C. After 1 h of incubation, the cells were washed twice with PBS and overlaid with MEM containing 1% agarose. After 48 h of incubation at 37°C, the agarose was removed, and the cells were stained with 0.5% crystal violet in 10% formaldehyde solution. The plaques were visualized and manually counted.

Hemagglutination–elution assay

Hemagglutination–elution assay was adapted from a previously described procedure.⁶⁵ H5N6 influenza viruses were adsorbed to a 1% suspension of chicken and guinea pig erythrocytes at 4 °C for 30 min, and the HA titres at 37 °C representing viral elution from chicken and guinea pig erythrocytes was monitored every hour for 8 h. The HA titres following incubation at 37 °C was recorded as the percentage of the HA titres at time zero at 4 °C. Three independent experiments were performed.

Thermostability assay

The thermostability of the H5N6 viruses was measured by determining the loss of the viral titres after incubating the viruses at 55 °C temperature for 1–5 h with the original titres of 64 HAU. The titres of heat-treated H5N6 viruses were determined by HA assay. Three independent experiments were performed.

Construction and eukaryotic expression of plasmids

The eukaryotic expression vector pPRE, kindly provided by Dr. Feng Li (South Dakota State University, USA), was used with both the cytomegalovirus (CMV) immediate-early promoter and the bovine growth hormone polyadenylation signal controlled. The full sequence map for the eukaryotic expression vector pPRE was available from [Figure S3](#). The pPRE-674-272N-Flag, pPRE-674-272D-Flag, pPRE-YN-9-272N-Flag, and pPRE-YN-9-272D-Flag plasmids were constructed by digesting pPRE-Flag plasmid with XhoI and NotI restriction endonucleases. The pPRE-674-272N-Flag and pPRE-674-272D-Flag plasmids contained the amino acid N and D, respectively, in the NA gene of the A/duck/Guangdong/674/2014 (H5N6) virus. The pPRE-YN-9-272N-Flag and pPRE-YN-9-272D-Flag plasmids contained the amino acid N and D, respectively, in the NA gene of the A/duck/Yunnan/YN-9/2016 (H5N6) virus.⁴²

HEK293T cell monolayers in 6-well plates were transfected at 80–90% confluency with 4 µg of the pPRE-674-272N-Flag, pPRE-674-272D-Flag, pPRE-YN-9-272N-Flag, and pPRE-YN-9-272D-Flag plasmids using Lipofectamine 2000 (Invitrogen) according to the manufacturer's instructions. DNA and transfection reagent

were mixed and incubated at room temperature for 20 min and added to the cells. After 4 hours, the mixture was replaced with Opti-MEM (GIBCO) containing 0.2% BSA. After 48 hours, proteins from the cell cultures were separated on 8% SDS-PAGE gels and electrotransferred onto nitrocellulose membranes. Monoclonal mouse anti-FLAG (F3165, Sigma) was used to detect NA; whereas monoclonal mouse anti-GAPDH (HC301, Transgen) was used to detect GAPDH. Goat anti-rabbit or mouse IgG conjugated with horseradish peroxidase (1:10,000 dilution for 30 min at room temperature; Dingguo, Beijing, China) was used as a secondary antibody, followed by chemiluminescence detection (Odyssey Imaging System, LI-COR).

Neuraminidase activity assay

NA enzymatic activity assay was performed as described previously.⁶⁶ HEK293T cell monolayers in 12-well plates were transfected at 80–90% confluency with 2 μ g of the pPRE-674-272N-Flag, pPRE-674-272D-Flag, pPRE-YN-9-272N-Flag, and pPRE-YN-9-272D-Flag plasmids using Lipofectamine 2000 (Invitrogen) according to the manufacturer's instructions. DNA and transfection reagent were mixed and incubated at room temperature for 20 min and added to the cells. Four hours later, the mixture was replaced with Opti-MEM (GIBCO) containing 0.2% BSA. After 48 hours, HEK293T cells that express different NA were harvested by centrifugation and subsequently resuspended in the assay buffer containing 2% fetal bovine serum. The samples were analyzed using an NA assay kit (Beyotime Institute of Biotechnology, China). First, NA detection buffer was added in a volume of 70 μ L in a 96-well fluorescent enzyme labeling plate. Second, each NA sample was added with Milli-Q H₂O in volumes of 10 μ L and 10 μ L, respectively. Third and last, NA fluorescent substrate was added in a volume of 10 μ L, after which NA activity on the surface of cells was measured with a fluorescence microplate reader for 70 min at 37 °C. The substrate's cleavage due to NA activity produced fluorescence with an emission wavelength of 450 nm with an excitation wavelength of 322 nm. The intensity of fluorescence reflected the activity of NA from transfected HEK293T cells.

Indirect immunofluorescent assay

HEK293T cells were grown on cover slips in 24-well plates. After experimental treatment (i.e., transfection with 2 μ g plasmids for 24 h), cells were fixed in 4% paraformaldehyde for 30 min at room temperature, and later permeabilized and blocked with PBS containing 0.5% Triton-X-100 and 5% BSA for 1 h, also at room temperature. For immunostaining, samples were incubated with antibody against indicated antibodies for 2 h at room temperature or 4°C overnight, followed by incubation with anti-mouse IgG FITC-conjugated antibody or anti-rabbit IgG Alexa Fluor 594-conjugated antibody for 1 h. The nuclei of cells were visualized with 4',6-diamidino-2-phenylindole (DAPI; Invitrogen), and all fluorescence images were acquired with a confocal microscope (Olympus).

Luciferase reporter assay

In brief, we used a modified luciferase reporter plasmid previously described,²⁷ containing RNA polymerase I promoter, RNA polymerase I terminator, NA segment-derived noncoding region, and the firefly luciferase gene. The reporter plasmid was constructed by inserting different NA segments containing amino acids D, N, and S at position 272 of NA and corresponding mutations of amino acids D, N, and S at the same position. The reporter plasmid was constructed by inserting different NA sequence whose sequences were derived from the opening reading frame (ORF) of the NA gene in the 674 strain between a start codon and the remaining ORF of the firefly luciferase gene. To be specific, the different NA gene sequences contained amino acid D (i.e., GAC and GAT codon), N (i.e., AAC and AAT codon), and S (i.e., AGT, AGC, and TCC codon). The RNP complexes, consisting of 200 ng of each of the PA, PB1, PB2, and NP plasmids of the SH7 strain were mixed with a luciferase reporter plasmid (200 ng) and a thymidine kinase promoter-Renilla luciferase reporter plasmid (pRL_TK) construct (20 ng), followed by co-transfection into 293T cells in a 12-well plate with Lipofectamine 2000 (Invitrogen, Carlsbad, CA, USA) and incubation at 37 °C for 24 h. Luciferase production was assayed using the Dual-Luciferase Reporter Assay System (Promega) according to the manufacturer's instructions. Firefly luciferase activities were standardized to the transfection control of Renilla luciferase activities (i.e., firefly luciferase activities were divided by Renilla luciferase activities).

Quantitative real-time PCR (qRT-PCR)

Levels of mRNA, vRNA, and cRNA were determined in MDCK cells infected with H5N6 viruses. Total RNA was extracted from infected MDCK cells using an RNeasy Mini Kit (Qiagen) as directed by the manufacturer. Reverse transcription was performed using Moloney murine leukemia virus reverse transcriptase (M-MLV

RT, Takara) with either a random or strand-specific primer. Strand-specific primers were used to generate cDNAs from 0.5 μg of total RNA per sample using M-MLV RT. The strand-specific primer sequences (5'–3') that we used were available from [key resources table](#).

The qRT-PCR mixture for each reaction sample consisted of 10 μL of 2 \times SYBR PCR master mix (Vazyme Biotech Co., Ltd, China), 7 μL of nuclease-free water, 0.5 μL of each primer, and 2 μL of cDNA template. The expression of each gene was detected using the 7,500 Real-Time PCR System (Applied Biosystems) with one cycle at 95 $^{\circ}\text{C}$ for 10 min, followed by 40 cycles of 95 $^{\circ}\text{C}$ for 15 s and 60 $^{\circ}\text{C}$ for 1 min. Expression values of each gene, relative to GAPDH, were calculated using the $2^{-\Delta\Delta\text{CT}}$ method. Each experiment comprised three technical replicates for each sample, and three experimental replications were performed using the following primers (5'–3'). The primers of mRNA, vRNA, and cRNA were available from [key resources table](#).

In addition, A549 cells were infected with each H5N6 virus at an MOI of 1 for 1 h, followed by washing to remove unbound viruses and incubation in DMEM containing 0.2% BSA (Dingguo, Beijing, China) at 37 $^{\circ}\text{C}$ with 5% CO_2 for 24 h and 48 h. The mRNA levels of inflammatory cytokines IL-1 β , IL-6, IL-8, TNF- α , and IFN- β induced by H5N6 viral infection were detected using qPCR. Once total RNA was isolated using an RNeasy Mini Kit (Qiagen) as directed by the manufacturer, reverse transcription was performed using the PrimeScript RT Reagent Kit (Takara), also according to the manufacturer's instructions. The qRT-PCR mixture for each reaction sample consisted of 10 μL of 2 \times SYBR PCR master mix (Vazyme Biotech Co., Ltd, China), 7 μL of nuclease-free water, 0.5 μL of each primer, and 2 μL of cDNA template. The expression of each gene was detected using the 7500 Real-Time PCR System (Applied Biosystems) with one cycle at 95 $^{\circ}\text{C}$ for 10 min, followed by 40 cycles of 95 $^{\circ}\text{C}$ for 15 s and 60 $^{\circ}\text{C}$ for 1 min. Expression values of each gene, relative to GAPDH, were calculated using the $2^{-\Delta\Delta\text{CT}}$ method. The primers of inflammatory cytokine were available from [key resources table](#).

Select the appropriate model of NA protein stimulated by ColabFold and structure superposition and comparison

Each NA protein of 674–272D, 674–272N, and 674–272S had five stimulated models ranked by pLDDT.⁴¹ The structural similarity (RMSD) and pLDDT ranking were taken into consideration to choose the final model. The final three best-fit models of each group were used in the following analysis. The main structural difference of final models for NA protein of 674–272D, 674–272N, and 674–272S was the loop (~40–70 aa) area due to the low pLDDT of stimulation. Hence, we superposed structures (76–459 aa) of NA protein and the 272 amino acids of D, N, and S were further analyzed. We calculated the interaction of D272, N272, and S272 with their surrounding residues, respectively.

QUANTIFICATION AND STATISTICAL ANALYSIS

All data were presented as the means \pm the standard errors of means (SEMs). Student's t-test was utilized to compare the difference between different groups. Statistical significance was indicated as * ($p < 0.05$), ** ($p < 0.01$), *** ($p < 0.001$), **** ($p < 0.0001$). All statistical analyses and calculations were performed using GraphPad Prism 7.